

GraHTP: A Provable Newton-like Algorithm for Sparse Phase Retrieval

Licheng Dai[†], Xiliang Lu[‡], Juntao You^{*,§,¶}

[†]School of Mathematics and Statistics, Wuhan University
Wuhan 430072, China

[‡]School of Mathematics and Statistics, and Hubei Key Laboratory of Computational Science, Wuhan University
Wuhan 430072, China

[§]School of Artificial Intelligence, Wuhan University, Wuhan 430072, China

[¶]Institute for Advanced Study, Shenzhen University, Shenzhen 518000, China

Abstract—This paper investigates the sparse phase retrieval problem, which aims to recover a sparse signal from a system of quadratic measurements. In this work, we propose a novel non-convex algorithm, termed Gradient Hard Thresholding Pursuit (GraHTP), for sparse phase retrieval with complex sensing vectors. GraHTP is theoretically provable and exhibits high efficiency, achieving a quadratic convergence rate after a finite number of iterations, while maintaining low computational complexity per iteration. Numerical experiments further demonstrate GraHTP’s superior performance compared to state-of-the-art algorithms.

Index Terms—sparse phase retrieval, phaseless recovery, Gradient Hard Thresholding Pursuit, Gauss-Newton method, quadratic convergence.

I. INTRODUCTION

PHASE retrieval is to recover a signal from the squared modulus of its linear transform, which can be denoted as finding an n -dimensional signal \mathbf{x}^\dagger from a system of quadratic equations in the form

$$y_j = |\langle \mathbf{a}_j, \mathbf{x}^\dagger \rangle|^2, j = 1, \dots, m, \quad (\text{I.1})$$

where $\{y_j\}_{j=1}^m \subset \mathbb{R}_+^m$ are observed data, $\{\mathbf{a}_j\}_{j=1}^m \subset \mathbb{C}^n$ are given sensing vectors, and m is the number of measurements. The phase retrieval problem arises naturally in fields where direct phase acquisition is difficult or unattainable, such as optics [1], [2], X-ray crystallography [3], quantum mechanics [4], quantum information [5], and others [6]–[9].

Solving the nonlinear system (I.1) presents significant challenges. Without additional assumptions on \mathbf{x}^\dagger , the system (I.1) may have multiple solutions. Ensuring a unique solution (up to a global phase) requires the so-called “oversampling” (i.e. $m > n$) technique, where $m \geq 2n - 1$ for real signals and $m \geq 4n - 4$ for complex signals have been shown to be sufficient with generic sensing vectors [10], [11]. Developing practical algorithms for this problem is also highly challenging, which can be traced back to the classical works of Gerchberg-Saxton [12] and Fineup [13]. However, earlier approaches lacked rigorous theoretical guarantees. Despite NP-hardness of the problem, a number of practical algorithms that are guaranteed to find true signal (up to global phase) in probabilistic models

have been introduced in recent years, which can be categorized into convex and non-convex approaches. Typical convex approaches including PhaseLift [8], [14], PhaseCut [15], PhaseMax [16] and Flexible convex relaxation [17], enable to recovery signal exactly. However, they can be computationally expensive, especially those that use semi-definite programming (SDP) relaxation and lift the phase retrieval problem to higher dimensional space. Recent studies have introduced several non-convex approaches, including AltminPhase [18], Wirtinger flow [19], truncated amplitude flow (TAF) [20], Kaczmarz [21], [22], Riemannian optimization [23], Gauss-Newton methods [24], [25], among others. These algorithms typically require an initial guess that is sufficiently close to the ground truth to ensure successful recovery, for which the spectral initialization method and its various variants are commonly employed under random Gaussian measurements. Additionally, some approaches have been considered in the context of masked Fourier measurements [14], [26], [27]. The number of measurements required by these provable algorithms are $m \sim \mathcal{O}(n \log^a n)$ with $a \geq 0$, which is (nearly) optimal.

Nevertheless, there is significant interest in reducing the necessary number of measurements m , especially in high-dimensional applications. This requires leveraging additional information about the unknown signal. In many signal/image processing applications, it is well-established that natural signals or images are often (approximately) sparse in a transformed domain [28]. Assuming the n -dimensional target signal \mathbf{x}^\dagger is at most s -sparse, where $s \ll n$, leads to a sparse phase retrieval problem: recovering \mathbf{x}^\dagger from

$$y_j = |\langle \mathbf{a}_j, \mathbf{x}^\dagger \rangle|^2, j = 1, \dots, m, \quad \text{s.t.} \quad \|\mathbf{x}^\dagger\|_0 \leq s, \quad (\text{I.2})$$

where $\|\mathbf{x}^\dagger\|_0$ denotes the number of nonzero components in \mathbf{x}^\dagger . Sparse phase retrieval allows for the recovery of the target signal from an underdetermined system ($m < n$), making it possible to solve phase retrieval problem when only a small number of phaseless measurements are available in practice. It has been shown that $m = \mathcal{O}(s)$ generic measurements are sufficient to determine a unique solution [29], [30]. However, practical solvers for (I.2) face challenges due to the inherent non-linearity and non-smoothness, especially in underdetermined systems.

*Corresponding author: jyoub@connect.ust.hk.

A. Related Work and Our Contributions

The sparse phase retrieval problem (I.2) has been extensively studied in recent years, and a number of provable practical algorithms have been introduced. For instance, the ℓ_1 -regularized PhaseLift [31], a natural extension of the convex approach to the compressive case, demonstrates that the signal \mathbf{x}^\dagger can be correctly recovered with $\mathcal{O}(s^2 \log n)$ random Gaussian measurement. Non-convex algorithms have also garnered lots attention due to their computational efficiency. Non-convex approaches typically involve two stages: an initialization stage followed by a local refinement stage. Such algorithms include SPARTA [9], CoPRAM [32], thresholding/projected Wirtinger flow [33], [34], SAM [35], HTP [36] and others [37]. Given an initial guess sufficiently close to the target signal, most of these algorithms guarantee at least linear convergence to the ground truth with $\mathcal{O}(s \log(n/s))$ random Gaussian measurements. Meanwhile, an initial guess sufficiently close to the ground truth can be generated using specific methods, such as spectral methods, which can produce an appropriate initial guess using $m \sim \mathcal{O}(s^2 \log n)$ random Gaussian measurements [9], [18]. For a more detailed discussion, see [38].

Theoretically, algorithms like ThWF, SPARTA and CoPRAM achieve ϵ -accuracy in $\mathcal{O}(\log(1/\epsilon))$ iterations. Recently proposed methods such as HTP and SAM guarantee exact recovery of target signal within a finite number of iterations, specifically at most $\mathcal{O}(\log(s^2 \log n) + \log(\|\mathbf{x}^\dagger\|/x_{\min}^\dagger))$ iterations. This demonstrates improved efficiency in solving the sparse phase retrieval problem. However, these theories of finite-step convergence are based either on the case of real-valued \mathbf{x}^\dagger and $\{\mathbf{a}_j\}_{j=1}^m$, or on assumptions that certain problems on subspaces can be exactly solved [39]. It is known that complex sensing vectors $\{\mathbf{a}_j\}_{j=1}^m$ are of great interest in the applications [14]. In this work, we explore the scenario where the sensing vectors are complex and present a novel, efficient Newton-like algorithm which is guaranteed to achieve superlinear convergence. Our main contributions are four-fold:

- Gradient Hard Thresholding Pursuit (GraHTP) [40], [41] has demonstrated high efficiency in solving sparsity-constrained convex optimization problems. We extend the GraHTP framework to address compressive quadratic equations, where the fitting loss is nonconvex and the subspace problem lacks a straightforward exact solution.
- The proposed practical algorithm, GraHTP for sparse phase retrieval, is highly efficient. To find an ϵ -solution, the number of iterations is at most $\mathcal{O}(\log(\log(1/\epsilon)) + \log(\|\mathbf{x}^\dagger\|_2/x_{\min}^\dagger))$ with a per iteration complexity $\mathcal{O}(mn + s^2n)$. For $s \ll n$, the per-iteration complexity is of the same order as that of first-order gradient-type methods.
- The theoretical guarantee of quadratic convergence rate, achieved after at most $\mathcal{O}(\log(\|\mathbf{x}^\dagger\|/x_{\min}^\dagger))$ iterations, has been established for GraHTP under some mild conditions. As far as we know, theoretical analysis for practical algorithms in sparse phase retrieval problem with complex Gaussian random measurements are mostly linear.
- The empirical advantages of the proposed algorithm have

been verified against state-of-the-art algorithms. Numerical experimental results illustrate that GraHTP achieves the superior computational efficiency and recoverability in all test problems, including real case and complex case.

B. Notation

For an index set $\mathcal{S} \subseteq \{1, 2, \dots, n\}$, $|\mathcal{S}|$ denotes the number of elements in set \mathcal{S} . For a vector $\mathbf{z} \in \mathbb{R}^n$, $\|\mathbf{z}\|_2$ denotes the Euclidean norm. $\mathbf{z}_{\mathcal{S}}$ means the sub-vector indexed by \mathcal{S} . For a matrix $\mathbf{A} \in \mathbb{R}^{m \times n}$, $\|\mathbf{A}\|_2$ denotes the spectral norm, $\mathbf{A}_{\mathcal{S}}$ represents retaining only the columns of the matrix indexed by \mathcal{S} , and $\mathbf{A}_{\mathcal{S}, \mathcal{T}}$ represents retaining the columns and rows of the matrix indexed by \mathcal{S} and \mathcal{T} respectively. $\mathbf{I}_{|\mathcal{T}|}$ denotes the $|\mathcal{T}|$ dimensional identity matrix. Hard thresholding operator $\mathcal{H}_s : \mathbb{R}^n \rightarrow \mathbb{R}^n$ represents retaining the maximum s components in the magnitude of a vector in \mathbb{R}^n , and setting the other components to zero. x_{\min}^\dagger represents the nonzero component with the smallest absolute value of the vector \mathbf{x}^\dagger .

II. ALGORITHMS

In this section, we describe our proposed algorithm in detail. The proposed algorithm is based on the general framework of GraHTP [40], [41], which enjoys finite-step convergence in the case of compressive sensing [42]. And similar to most of the existing non-convex sparse phase retrieval algorithms, the proposed algorithm consists of two stages, namely, the initialization stage and the iterative refinement stage. In this work, we focus on the iterative refinement stage, and the initialization stage can be done by an off-the-shelf algorithm such as the spectral method or modified spectral method [38].

A. The Proposed Algorithm

In practice, the unknown signal can belong to \mathbb{R}^n or \mathbb{C}^n . For simplicity, we will consider $\mathbf{x}^\dagger \in \mathbb{R}^n$ in the following discussion. The squared error loss associated with (I.2), commonly referred to as the intensity-based loss in the context of the phase retrieval problem, naturally leads to the following optimization problem:

$$\min_{\mathbf{z} \in \mathbb{R}^n} f(\mathbf{z}), \text{ s.t. } \|\mathbf{z}\|_0 \leq s, \quad (\text{II.3})$$

where

$$f(\mathbf{z}) := \frac{1}{4m} \sum_{j=1}^m (|\langle \mathbf{a}_j, \mathbf{z} \rangle|^2 - y_j)^2. \quad (\text{II.4})$$

To address the problem formulated in (II.3), we consider employing the GraHTP method, as introduced in [40], [41]. GraHTP extends the HTP algorithm from compressed sensing to tackle the broader framework of sparsity-constrained convex optimization problems. The approach begins with a projected gradient descent (PGD), followed by subspace selection, and then resolves a subspace optimization problem to refine the solution. Specifically, for a given current estimate \mathbf{z}^k at the k -th iteration, the one-step update of \mathbf{z}^k consists of the following three sub-steps:

- 1) Compute the PGD update as

$$\mathbf{u}^k = \mathcal{H}_s(\mathbf{z}^k - \mu^k \nabla f(\mathbf{z}^k)), \text{ step size } \mu^k > 0. \quad (\text{II.5})$$

2) Estimate guess of the support

$$\mathcal{S}_{k+1} = \text{supp}(\mathbf{u}^k).$$

3) Compute update $\mathbf{z}^{k+1} = \hat{\mathbf{z}}^{k+1}$ where

$$\hat{\mathbf{z}}^{k+1} \leftarrow \arg \min_{\text{supp}(\mathbf{z}) \subseteq \mathcal{S}_{k+1}} f(\mathbf{z}). \quad (\text{II.6})$$

However, applying GraHTP directly to our problem is not feasible both algorithmically and theoretically. Firstly, the exact solution for the optimization problem (II.6) associated with the loss function in (II.4) is nontrivial to obtain. Moreover, ensuring convergence in the case of non-convex $f(\mathbf{z})$ and the lack of an exact solution for (II.6) pose significant challenges.

For the first issue, it is important to note that we are minimizing $f(\mathbf{z})$ on restricted supporting set \mathcal{S}_{k+1} , which is small in scale compared to the dimension n . Therefore, we propose solving (II.6) approximately with L steps of Gauss-Newton iteration [43], [44]. Let $\{\mathbf{z}^{k,l}\}_{l=0}^L$ be the sequence generated by the iteration with an initial guess $\mathbf{z}^{k,0}$. For example, one can choose the initial guess $\mathbf{z}^{k,0} = \mathbf{u}^k$. Next we perform Gauss-Newton update. For the ease of notation, we let $F_j(\mathbf{z}) := \frac{1}{2\sqrt{m}}(|\langle \mathbf{a}_j, \mathbf{z} \rangle|^2 - y_j)$ as the j -th component of $\mathbf{F}(\mathbf{z}) : \mathbb{R}^n \rightarrow \mathbb{R}^m$, and the loss function $f(\mathbf{z})$ can be written in the form of:

$$f(\mathbf{z}) = \sum_{j=1}^m F_j(\mathbf{z})^2. \quad (\text{II.7})$$

Performing a first-order Taylor expansion of $\mathbf{F}(\mathbf{z})$ at $\mathbf{z}^{k,l}$:

$$\mathbf{F}(\mathbf{z}) \approx \mathbf{F}(\mathbf{z}^{k,l}) + \mathbf{J}(\mathbf{z}^{k,l})(\mathbf{z} - \mathbf{z}^{k,l}), \quad (\text{II.8})$$

where the j -th row of matrix $\mathbf{J}(\mathbf{z}^{k,l}) \in \mathbb{R}^{m \times n}$ is $\frac{1}{\sqrt{m}}(\mathbf{a}_{jR} \mathbf{a}_{jR}^\top \mathbf{z}^{k,l} + \mathbf{a}_{jI} \mathbf{a}_{jI}^\top \mathbf{z}^{k,l})^\top$ and \mathbf{a}_{jR} , \mathbf{a}_{jI} are the real and imaginary part of \mathbf{a}_j respectively. Combining with (II.7), the problem in (II.6) can be approximated by

$$\min_{\text{supp}(\mathbf{z}) \subseteq \mathcal{S}_{k+1}} \|\mathbf{J}(\mathbf{z}^{k,l})(\mathbf{z} - \mathbf{z}^{k,l}) + \mathbf{F}(\mathbf{z}^{k,l})\|_2^2. \quad (\text{II.9})$$

Denote $\mathbf{z}^{k,l+1}$ as the solution to (II.9), which satisfies

$$\mathbf{z}_{\mathcal{S}_{k+1}^c}^{k,l+1} = \mathbf{0}$$

and

$$\begin{aligned} & \mathbf{J}_{\mathcal{S}_{k+1}}(\mathbf{z}^{k,l})^\top \mathbf{J}_{\mathcal{S}_{k+1}}(\mathbf{z}^{k,l})(\mathbf{z}_{\mathcal{S}_{k+1}}^{k,l} - \mathbf{z}_{\mathcal{S}_{k+1}}^{k,l+1}) \\ &= \mathbf{J}_{\mathcal{S}_{k+1}}(\mathbf{z}^{k,l})^\top \mathbf{F}(\mathbf{z}^{k,l}). \end{aligned} \quad (\text{II.10})$$

Finally we choose the update \mathbf{z}^{k+1} as $\mathbf{z}^{k,L}$. The proposed algorithm, coined GraHTP for sparse phase retrieval, is summarized in Algorithm 1. Also, the proposed algorithm can be extended to the case of complex \mathbf{x}^\dagger .

For the proposed GraHTP, computing $\mathbf{z}^{k,0}$ and \mathbf{z}^{K+1} costs $\mathcal{O}(mn)$ and $\mathcal{O}(s^2m)$ flops, respectively. The total computational cost for updating \mathbf{z} in Algorithm 1 is $\mathcal{O}(mn + s^2m)$ per iteration. As long as $s \ll n$ or $s \leq \sqrt{n}$, the per-iteration complexity of the proposed algorithm is comparable to that of first-order gradient-type methods like thresholding/projected Wirtinger flow [33], [34], which also costs $\mathcal{O}(mn)$ flops per-iteration. However, our proposed algorithm guarantees super-linear convergence under certain conditions, as established in the next section.

Algorithm 1 Gradient Hard Thresholding Pursuit for Sparse Phase Retrieval

Input: Data $\{\mathbf{a}_j, y_j\}_{j=1}^m$, the sparsity level s , the maximum number K and L of iterations allowed, step size μ^k .

- 1: Initialization: Let the initial value \mathbf{z}^0 be generated by a given method, e.g., (modified) spectral method [32], [38].
- 2: **for** $k = 0, 1, \dots, K - 1$ **do**
- 3: $\mathbf{u}^k = \mathcal{H}_s(\mathbf{z}^k - \mu^k \nabla f(\mathbf{z}^k))$
- 4: $\mathcal{S}_{k+1} = \text{supp}(\mathbf{u}^k)$
- 5: Obtain \mathbf{z}^{k+1} by solving

$$\min_{\text{supp}(\mathbf{z}) \subseteq \mathcal{S}_{k+1}} \sum_{j=1}^m F_j(\mathbf{z})^2$$

via L steps of Gauss-Newton iteration: starting from $\mathbf{z}^{k,0}$ where $\text{supp}(\mathbf{z}^{k,0}) = \mathcal{S}_{k+1}$ (e.g., $\mathbf{z}^{k,0} = \mathbf{u}^k$),

for $l = 0, \dots, L - 1$ **do**

$$\mathbf{z}^{k,l+1} = \arg \min_{\text{supp}(\mathbf{z}) \subseteq \mathcal{S}_{k+1}} \|\mathbf{J}(\mathbf{z}^{k,l})(\mathbf{z} - \mathbf{z}^{k,l}) + \mathbf{F}(\mathbf{z}^{k,l})\|_2^2$$

end for

Set $\mathbf{z}^{k+1} = \mathbf{z}^{k,L}$

6: **end for**

Output: $\mathbf{z}_{\text{output}} = \mathbf{z}^K$.

B. Theoretical Results

In this subsection, we present the theoretical results of the proposed GraHTP for sparse phase retrieval as summarized in Algorithm 1. The distance between \mathbf{x}^\dagger and \mathbf{z} is define as $\text{dist}(\mathbf{x}^\dagger, \mathbf{z}) := \min\{\|\mathbf{x}^\dagger - \mathbf{z}\|_2, \|\mathbf{x}^\dagger + \mathbf{z}\|_2\}$ as \mathbf{x}^\dagger and $-\mathbf{x}^\dagger$ are equivalent solutions. If the current guess \mathbf{z}^k fall within a nearby local neighborhood of \mathbf{x}^\dagger or $-\mathbf{x}^\dagger$, the following Theorem II.1 demonstrates the one-step contraction property of GraHTP in Algorithm 1 with $L = 1$, referring to the number of Gauss-Newton iterations. For ease of presentation, we denote the basin of attraction as

$$\mathcal{E}(\delta_0) := \{\mathbf{z} \in \mathbb{R}^n \mid \text{dist}(\mathbf{z}, \mathbf{x}^\dagger) \leq \delta_0 \|\mathbf{x}^\dagger\|_2, \|\mathbf{z}\|_0 \leq s\}.$$

for $\delta_0 \geq 0$.

Theorem II.1. *Let $\mathbf{x}^\dagger \in \mathbb{R}^n$ be any s -sparse signal. Consider m noiseless measurements $y_j = |\langle \mathbf{a}_j, \mathbf{x}^\dagger \rangle|^2$ from i.i.d. $\mathbf{a}_j \sim \mathcal{CN}(\mathbf{0}, \mathbf{I})$, $j = 1, 2, \dots, m$. Then, there exist positive constants $\mu_1, \mu_2, \delta, C_1, C_2, C_3, C_4$, $\rho \in (0, 1)$, $\alpha \in (0, 1)$ and β such that: For any fixed $\mathbf{z}^k \in \mathcal{E}(\delta)$, with probability at least $1 - C_1 m^{-1} - C_2 \exp(-C_3 m / \log m)$ we have*

a.) \mathbf{u}^k produced by Algorithm 1 satisfies

$$\text{dist}(\mathbf{u}^k, \mathbf{x}^\dagger) \leq \rho \cdot \text{dist}(\mathbf{z}^k, \mathbf{x}^\dagger),$$

b.) \mathbf{z}^{k+1} produced by Algorithm 1 with $L = 1$ and any fixed initial guess $\mathbf{z}^{k,0}$ with $\text{dist}(\mathbf{z}^{k,0}, \mathbf{x}^\dagger) \leq \text{dist}(\mathbf{u}^k, \mathbf{x}^\dagger)$ satisfies

$$\text{dist}(\mathbf{z}^{k+1}, \mathbf{x}^\dagger) \begin{cases} \leq \alpha \cdot \text{dist}(\mathbf{z}^k, \mathbf{x}^\dagger), \\ \leq \beta \cdot \text{dist}^2(\mathbf{z}^k, \mathbf{x}^\dagger), \quad \text{if } \mathbf{z}^k \in \mathcal{E}\left(\frac{\alpha \|\mathbf{x}^\dagger\|_2}{\|\mathbf{x}^\dagger\|_2}\right) \end{cases}$$

provided $\mu^k \in \left(\frac{\mu_1}{\|\mathbf{x}^\dagger\|_2^2}, \frac{\mu_2}{\|\mathbf{x}^\dagger\|_2^2}\right)$ and $m \geq C_4 s \log(n/s)$.

Proof. The proof of this theorem is deferred to Section IV-B and Section IV-C. \square

In fact, part a.) of Theorem II.1 demonstrates that the intensity-based loss minimized by the projected gradient descent method as in (II.5) exhibits linear convergence when appropriately initialized. Meanwhile, Part b.) of Theorem II.1 demonstrates that with proper starting guesses \mathbf{z}^k and $\mathbf{z}^{k,0}$, the proposed algorithm exhibits superlinear convergence.

Noticing that we can set $\mathbf{z}^{k,0} = \mathbf{u}^k$ to fulfill the requirement $\text{dist}(\mathbf{z}^{k,0}, \mathbf{x}^\dagger) \leq \text{dist}(\mathbf{u}^k, \mathbf{x}^\dagger)$. Then, Part b.) of Theorem II.1 suggests that locally Algorithm 1 exhibits two phases of convergence: initially, in the first phase, a linear rate of convergence is achieved when the current estimate is within an $\mathcal{O}(1)\|\mathbf{x}^\dagger\|_2$ neighborhood of \mathbf{x}^\dagger ; subsequently, in the second phase, the algorithm attains a quadratic convergence rate when the current estimate is within an x_{\min}^\dagger neighborhood of $\pm\mathbf{x}^\dagger$. Despite the dependency, the linear convergence achieved in the initial phase ensures that reaching x_{\min}^\dagger -closeness to $\pm\mathbf{x}^\dagger$ typically requires at most $\mathcal{O}(\log(\|\mathbf{x}^\dagger\|_2/x_{\min}^\dagger))$ iterations. Consequently, the proposed algorithm realizes a quadratic convergence rate after at most $\mathcal{O}(\log(\|\mathbf{x}^\dagger\|_2/x_{\min}^\dagger))$ iterations. The dependence can be technically addressed by a resampling or partition, and then we can achieve an ϵ -solution in at most $\mathcal{O}(\log(\log(1/\epsilon)) + \log(\|\mathbf{x}^\dagger\|_2/x_{\min}^\dagger))$ iterations, as stated in the following corollary.

Corollary II.1. *Let $\mathbf{x}^\dagger \in \mathbb{R}^n$ be any s -sparse signal and $\{\mathbf{a}_j, y_j\}_{j=1}^m$ generated as in Theorem II.1 be divided equally into $2K$ disjoint partitions $\{\mathbf{a}_j, y_j\}_{j \in \mathcal{I}_k}$, $k = 1, 2, \dots, 2K$. In the k -th iteration of Algorithm 1, use the data $\{\mathbf{a}_j, y_j\}_{j \in \mathcal{I}_{2k-1}}$ to estimate \mathbf{u}^k , and $\{\mathbf{a}_j, y_j\}_{j \in \mathcal{I}_{2k}}$ to estimate \mathbf{z}^{k+1} . Then, for some $K \leq \mathcal{O}(\log(\log(1/\epsilon)) + \log(\|\mathbf{x}^\dagger\|_2/x_{\min}^\dagger))$, there exist positive constants $\mu_1, \mu_2, \delta, C_5, C_6, C_7, C_8$ such that: If provided $\mu^k \in (\frac{\mu_1}{\|\mathbf{x}^\dagger\|_2^2}, \frac{\mu_2}{\|\mathbf{x}^\dagger\|_2^2})$, $m \geq C_5 K s \log(n/s)$ and $\mathbf{z}^0 \in \mathcal{E}(\delta)$, then with probability at least $1 - K(C_6 m^{-1} - C_7 \exp(-C_8 m / \log m))$, we have an ϵ -solution \mathbf{z}^K , i.e.,*

$$\text{dist}(\mathbf{z}^K, \mathbf{x}^\dagger) \leq \epsilon \|\mathbf{x}^\dagger\|_2.$$

Proof. The proof of this corollary is deferred to Section IV-D. \square

Nevertheless, we emphasize that the partition serves purely as a technical aid for analysis. Now we consider the noisy case that the measurements are given by $\mathbf{y}^{(\epsilon)} = \mathbf{y} + \boldsymbol{\varepsilon}$, where $\boldsymbol{\varepsilon} \in \mathbb{R}^m$ is a noise vector that independent of $\{\mathbf{a}_j\}_{j=1}^m$.

Theorem II.2. *Let $\mathbf{x}^\dagger \in \mathbb{R}^n$ be any s -sparse signal. Consider m noisy measurements $y_j^{(\epsilon)} = |\langle \mathbf{a}_j, \mathbf{x}^\dagger \rangle|^2 + \varepsilon_j$ from i.i.d. $\mathbf{a}_j \sim \mathcal{CN}(\mathbf{0}, \mathbf{I})$, $j = 1, 2, \dots, m$. Then, there exist positive constants $\mu_1, \mu_2, \delta, \eta, \zeta, \gamma, p, C, C'_1, C'_2, C'_3, C'_4$ and $\rho, \xi \in (0, 1)$ such that: For any fixed $\mathbf{z}^k \in \mathcal{E}(\delta)$, if $\|\boldsymbol{\varepsilon}\| \leq C \|\mathbf{x}^\dagger\|_2 x_{\min}^\dagger$, with probability at least $1 - C'_1 m^{-1} - C'_2 \exp(-C'_3 m / \log m)$*

a.) \mathbf{u}^k produced by Algorithm 1 satisfies

$$\text{dist}(\mathbf{u}^k, \mathbf{x}^\dagger) \leq \rho \cdot \text{dist}(\mathbf{z}^k, \mathbf{x}^\dagger) + p \cdot \|\boldsymbol{\varepsilon}\|_2,$$

b.) \mathbf{z}^{k+1} produced by Algorithm 1 with $L = 1$ and any fixed initial guess $\mathbf{z}^{k,0}$ with $\text{dist}(\mathbf{z}^{k,0}, \mathbf{x}^\dagger) \leq \text{dist}(\mathbf{u}^k, \mathbf{x}^\dagger)$ satisfies

$$\text{dist}(\mathbf{z}^{k+1}, \mathbf{x}^\dagger) \begin{cases} \leq \xi \cdot \text{dist}(\mathbf{z}^k, \mathbf{x}^\dagger) + \eta \cdot \|\boldsymbol{\varepsilon}\|_2, \\ \leq \zeta \cdot \text{dist}^2(\mathbf{z}^k, \mathbf{x}^\dagger) + \gamma \cdot \|\boldsymbol{\varepsilon}\|_2, \text{ if } \mathbf{z}^k \in \mathcal{E}(\frac{x_{\min}^\dagger}{\|\mathbf{x}^\dagger\|_2}) \end{cases}$$

provided $\mu^k \in (\frac{\mu_1}{\|\mathbf{x}^\dagger\|_2^2}, \frac{\mu_2}{\|\mathbf{x}^\dagger\|_2^2})$ and $m \geq C'_4 s \log(n/s)$.

Proof. The proof of this theorem is deferred to Section IV-E. \square

C. Initialization

The desired initial guess can be produced by algorithms such as spectral method or modified spectral method in the case of random Gaussian measurements. Spectral initialization method and its variants are often used in non-convex phase retrieval approaches to generate an initial guess. The spectral initialization constructs a matrix $\mathbf{Y} := \frac{1}{m} \sum_{i=1}^m y_i \mathbf{a}_i \mathbf{a}_i^*$ or its variants [18], [19], [45], whose leading eigenvector is a good approximation to $\pm\mathbf{x}^\dagger$ if provided the number of Gaussian measurements is at least $\mathcal{O}(n)$. For sparse phase retrieval, the number of Gaussian measurements for spectral initialization can be reduced by first estimating the guess of support of \mathbf{x}^\dagger as \mathcal{S}_0 , e.g., top- s entries in the diagonal elements of \mathbf{Y} given by $\{\frac{1}{m} \sum_{i=1}^m y_i a_{ij}^2\}_{j=1}^n$, and then the support vector of the initial guess is estimated as the principal eigenvector of $\frac{1}{m} \sum_{i=i}^m y_i [\mathbf{a}_i]_{\mathcal{S}_0} [\mathbf{a}_i]_{\mathcal{S}_0}^*$. The initial guess \mathbf{z}^0 generated by this setting can be sufficiently close to the ground truth: For any $\delta \in (0, 1)$, with probability at least $1 - 8m^{-1} \epsilon$ we have

$$\text{dist}(\mathbf{z}^0, \mathbf{x}^\dagger) \leq \delta \|\mathbf{x}^\dagger\|_2$$

provided $m \geq \mathcal{O}(s^2 \log n)$, see [32]. Moreover, the number of measurements required for the initialization stage can be further reduced by a modified version of spectral initialization. For more details, refer to [38].

III. NUMERICAL EXPERIMENTS

In our numerical simulation process, the true signal \mathbf{x}^\dagger is set to have s nonzero entries. In the first and second subsection, the sensing vectors $\{\mathbf{a}_j\}_{j=1}^m$ follow the Gaussian random distribution, i.e., $\mathbf{a}_j \sim \mathcal{CN}(\mathbf{0}, \mathbf{I})$. In the last subsection, we use partial discrete Fourier transform matrix as the sensing matrix $\mathbf{A} = [\mathbf{a}_1, \mathbf{a}_2, \dots, \mathbf{a}_m]^\top \in \mathbb{C}^{m \times n}$. The support set of \mathbf{x}^\dagger is uniformly and randomly extracted from all s -subsets of set $\{1, 2, \dots, n\}$ and the values of nonzero terms is independently and randomly generated from standard Gaussian distribution $\mathcal{N}(0, \mathbf{I})$. $\{y_j\}_{j=1}^m$ are samples without noise, where $y_j = |\langle \mathbf{a}_j, \mathbf{x}^\dagger \rangle|^2$, $j = 1, 2, \dots, m$. The observation datas with noise are defined by the following equation:

$$y_j^{(\epsilon)} = y_j + \sigma \varepsilon_j, \quad j = 1, \dots, m$$

where the noise $\{\varepsilon_j\}_{j=1}^m$ following the standard Gaussian random distribution, and we use $\sigma > 0$ to determine the noise level.

We will compare our algorithm GraHTP with other popular algorithms such as CoPRAM [32], ThWF [33], SPARTA

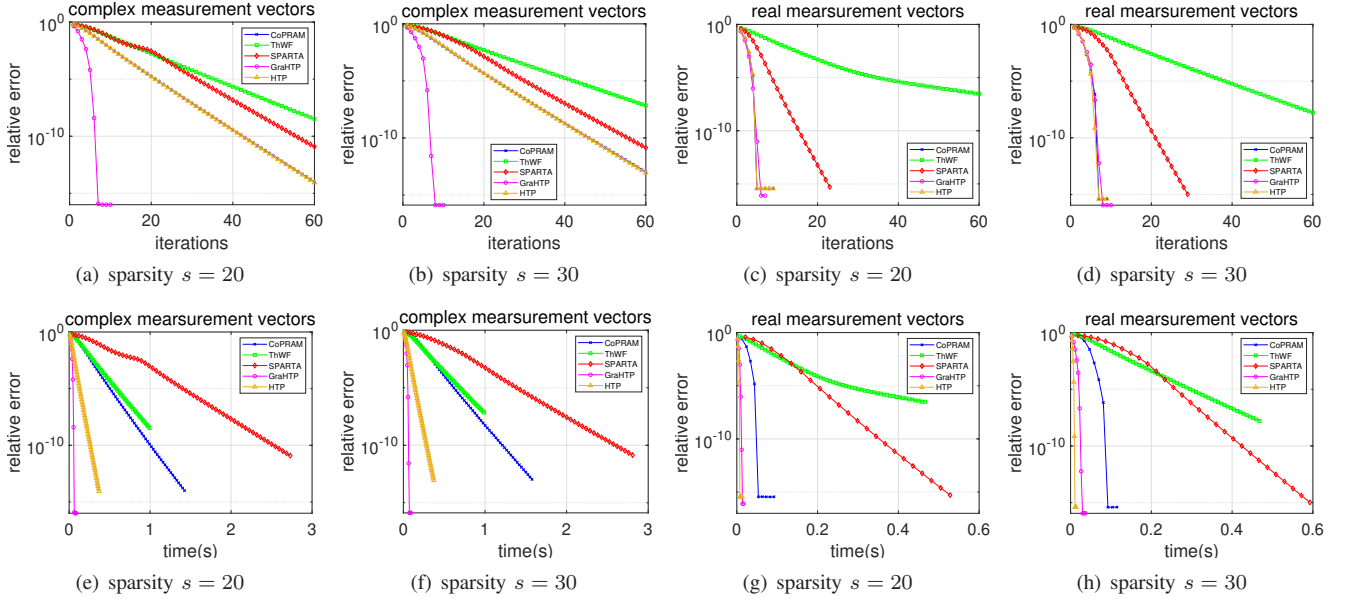


Fig. 1. Relative error versus number of iterations ((a)-(d)) and relative error versus running time ((e)-(h)) for CoPRAM, ThWF, SPARTA, HTP and our algorithm GraHTP, with fixed signal dimension $n = 3000$ and sample size $m = 2000$. The results represent the average of 100 independent trial runs.

[9] and HTP [36]. The numerical experiments are run on a computer with 3.00 GHz Intel Core i9 processor and 64 GB RAM using MATLAB R2023a. In experiments, the parameters of SPARTA are set to be $\mu = 1$, $\delta = 0.7$ and $|\mathcal{I}| = \lceil m/6 \rceil$ and the step size μ of HTP is fixed to be 0.95. The relative error between the true signal \mathbf{x}^\dagger and the estimated signal $\hat{\mathbf{x}}$ is defined as

$$r(\hat{\mathbf{x}}, \mathbf{x}^\dagger) = \frac{\text{dist}(\hat{\mathbf{x}}, \mathbf{x}^\dagger)}{\|\mathbf{x}^\dagger\|_2}. \quad (\text{III.11})$$

where $\text{dist}(\hat{\mathbf{x}}, \mathbf{x}^\dagger) = \min_{\phi \in [0, 2\pi)} \|\hat{\mathbf{x}} - e^{i\phi} \mathbf{x}^\dagger\|_2$. We define that signal recovery is successful when $r(\hat{\mathbf{x}}, \mathbf{x}^\dagger) \leq 10^{-6}$. For a fair comparison, the initial guess of GraHTP is generated using the spectral method described in [32].

A. Real-valued Signal Case

We first give the results of the numerical experiments under the case of real-valued signal.

Relative error. In this experiment, we compare the number of iterations and the running time required for different algorithms under the cases where sensing vectors are complex-valued and real-valued respectively. The experimental results depicted in Figure 1. The signal dimension is fixed to be $n = 3000$, the sample size is fixed to be $m = 2000$, the sparsity of true signal is set to be $s = 20$ and $s = 30$ respectively and the maximum number of iterations for each algorithm is 60. The x axis in the figure represents the iterations, and the y axis represents the relative error. We see that the number of iterations of our proposed algorithm for achieving $r(\hat{\mathbf{x}}, \mathbf{x}^\dagger) \leq 10^{-15}$ is fewer than other algorithms under the case where sensing vectors are complex-valued and that under the case where sensing vectors are real-valued is almost the same with CoPRAM and HTP and better than SPARTA and ThWF. The time of our algorithm for achieving

$r(\hat{\mathbf{x}}, \mathbf{x}^\dagger) \leq 10^{-15}$ is less than other algorithms when sensing vectors are complex-valued.

Running time comparison. We compare the proposed algorithm GraHTP with several algorithms in terms of running time for successful recovery ($r(\hat{\mathbf{x}}, \mathbf{x}^\dagger) \leq 10^{-6}$). In the experiment, the sample size m is fixed to be 2120, the sparsity is fixed to be 20, and the true signal dimension vary from $2^{10} \sim 2^{16}$. The results without those fail trials are shown in the Figure 2, the x axis in this figure represents the dimension n , and the y axis represents the average time of computations. According to the experiment, our algorithm GraHTP has better efficiency performance than others.

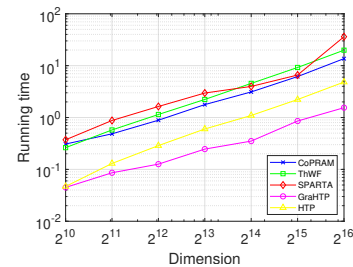


Fig. 2. Running time for successful recovery versus signal dimension for CoPRAM, ThWF, SPARTA, HTP and our algorithm GraHTP, with fixed sample size $m = 2120$ and sparsity 20. All results were obtained by averaging 100 independent experiments with those fail trials filtered out.

Phase transition. We present the results of comparing the recovery success rate of our algorithm GraHTP with other algorithms in Figures 3 and 4, and we see that our algorithm GraHTP performs better than other algorithms. In the first experiment, the dimension of true signal is fixed to be $n = 3000$, the sparsity is fixed to be $s = 20$ and $s = 30$ respectively, and the sample size m vary from $250 \sim 3000$. The result is plotted in Figure 3, the x axis represents the sample size m , and the y axis represents the successful recovery rate. In the second

experiment, the signal dimension is fixed to be $n = 3000$, the sparsity s vary from $10 \sim 80$ with grid size 5, and the sample size m vary from $250 \sim 3000$ with grid size 250. The grey level of a block means the success recovery rate under the given sparsity and sample size.

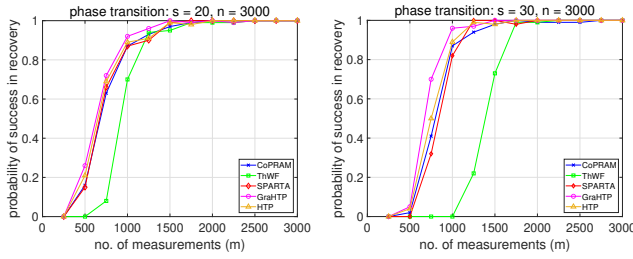


Fig. 3. Phase transition for algorithm CoPRAM, ThWF, SPARTA, HTP and our algorithm GraHTP, the results were obtained by averaging 100 independent experiments.

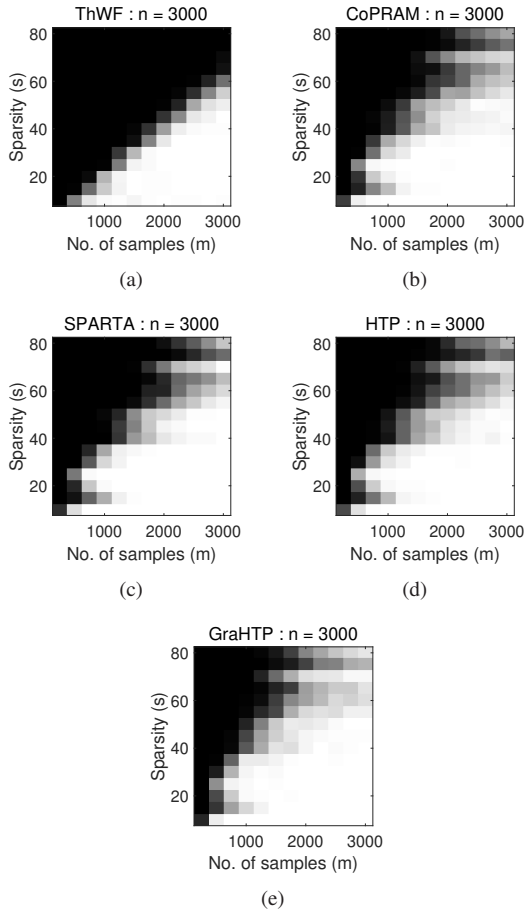


Fig. 4. Phase transition for algorithm CoPRAM, ThWF, SPARTA, HTP and our algorithm GraHTP, white block means 100% successful recovery, black block means 0% successful recovery and grey block means the rate of successful recovery between 0% and 100%. The results were obtained by averaging 100 independent experiments.

1-D signal reconstruction. Now we test the performance of different algorithms on recovering a 1-D signal from phaseless noisy measurements, the results of which are shown in Figure 5. The sampling matrix \mathbf{A} is of size 2800×8000 and it constructed from a complex random Gaussian matrix and

an inverse wavelet transform (with four level of Daubechies 1 wavelet). The noise level is $\sigma = 0.05$. The signal is sparse (73 nonzeros) induced in the wavelet transformation and we set s to be 80 in the numerical experiment since the exact sparsity level is unknown in practical. The PSNR values is defined as

$$\text{PSNR} = 10 \cdot \log \frac{V^2}{\text{MSE}}$$

where V represents the peak of the true signal, and MSE is the mean squared error of the signal reconstruction. The result shows that our proposed algorithm GraHTP cost less time to achieve the higher PSNR in signal reconstruction.

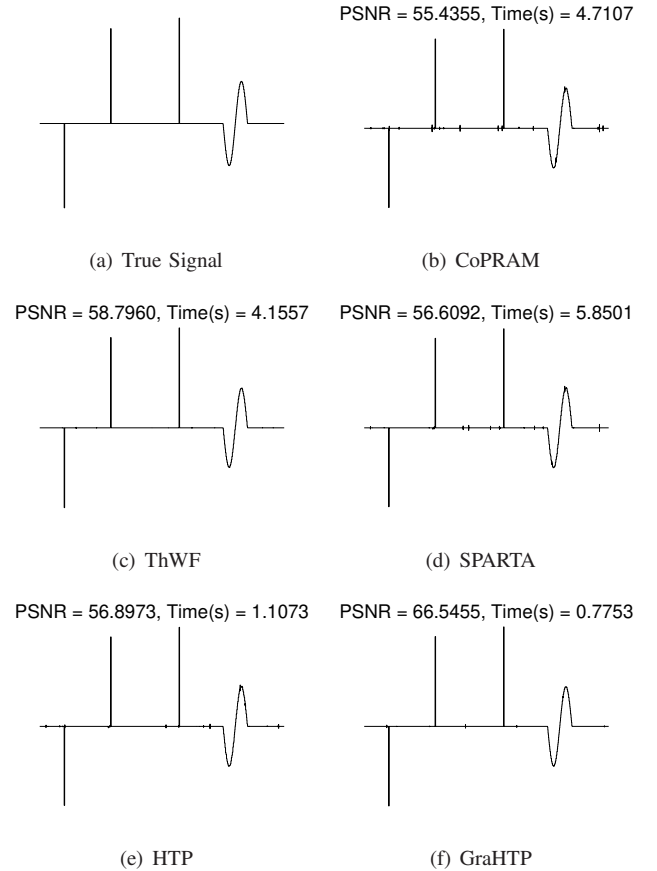


Fig. 5. 1-D signal reconstruction of algorithm CoPRAM, ThWF, SPARTA, HTP and our algorithm GraHTP. PSNR represents peak signal-to-noise ratio and Time(s) is the running time in seconds.

2-D image reconstruction. Figure 6 compares the performances of different algorithms on recovering a 2-D image (of size 64×64) with induced sparsity in the wavelet transform domain from noisy phaseless measurements. We use an thresholded wavelet transform (with four level of Daubechies 1 wavelet) of this image (contains 382 nonzeros) as the target signal. The noise level in the measurements is set to be $\sigma = 0.03$. The matrix \mathbf{A} is a complex random Gaussian matrix of size 3600×4096 . In the numerical experiment, the exact sparsity level is assumed to be unknown and sparsity s is set to be 400 for image reconstruction. We can see that in this experiment the PSNR of our proposed algorithm is higher than other methods.

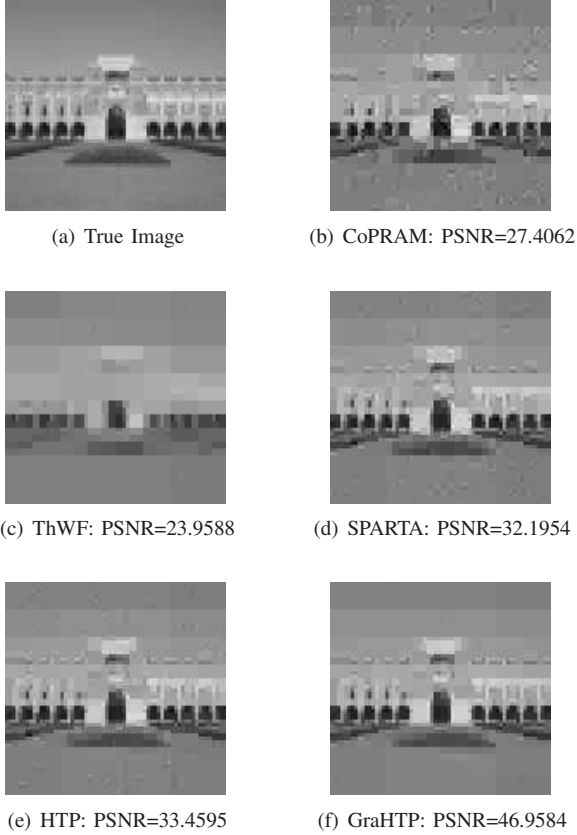


Fig. 6. 2-D image reconstruction of algorithm CoPRAM, ThWF, SPARTA, HTP and our algorithm GraHTP.

B. Complex-valued Signal Case

Next we will give the results of the numerical experiments for our proposed algorithm GraHTP under the case of complex-valued signal.

Relative error. We compare different algorithms under the case where the true signal and sensing vectors are all complex-valued, the experimental results in Figure 7 show the convergence of different algorithms. In this experiment the signal dimension is fixed to be $n = 3000$, the sample size is fixed to be $m = 2000$ and the sparsity is set as $s = 20$ and $s = 30$ respectively. The maximum number of iterations for each algorithm is 60. The x axis in the figure represents the iterations, and the y axis represents the relative error. According to this experiment, we can see that our algorithm GraHTP requires fewer iterations while achieving higher accuracy than others.

Phase transition. We present the results of comparing the recovery success ($r(\hat{x}, x^\dagger) \leq 10^{-6}$) rate of several algorithms in Figure 8. In this experiment, the true signal dimension is fixed to be $n = 3000$, the sparsity is fixed to be $s = 20$, and the corresponding sample sizes m vary from 250 \sim 3000. The x axis in the figure represents the sample size m , and the y axis represents the successful reconstruction rate.

C. Partial Discrete Fourier Transform Matrix

Relative error. In this experiment, we compare the number of iterations required for our proposed algorithm GraHTP

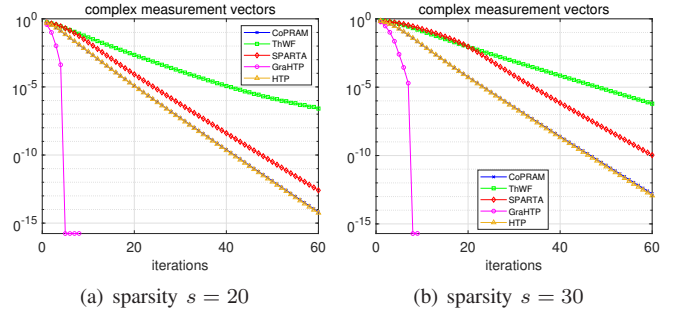


Fig. 7. Relative error versus number of iterations for CoPRAM, ThWF, SPARTA, HTP and our algorithm GraHTP, with fixed signal dimension $n = 3000$ and sample size $m = 2000$. The results represent the average of 100 independent trial runs.

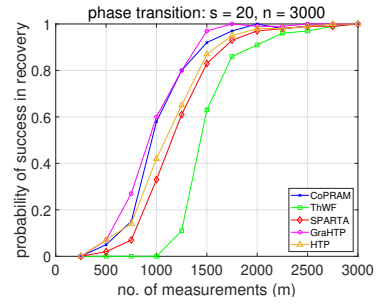


Fig. 8. Phase transition for algorithm CoPRAM, ThWF, SPARTA, HTP and our algorithm GraHTP, the results were obtained by averaging 100 independent experiments.

under the case where the sensing matrix A is a partial Discrete Fourier Transform (DFT) matrix, and the true signal is real-valued. We randomly generate an initial guess z^0 satisfying $r(z^0, x^\dagger) \leq 0.8$ as the input of our algorithm, and we construct the $m \times n$ sensing matrix by randomly selecting m rows of the $n \times n$ Discrete Fourier transform matrix. The experimental results depicted in Figure 9. The signal dimension is fixed to be $n = 2000$, the sample size is fixed to be $m = 1500$, the sparsity of true signal is set to be $s = 20$ and $s = 30$ respectively and the maximum number of iterations is 10. The x axis in the figure represents the iterations, and the y axis represents the relative error. We see that our proposed algorithm only need a few number of iterations for achieving $r(\hat{x}, x^\dagger) \leq 10^{-15}$.

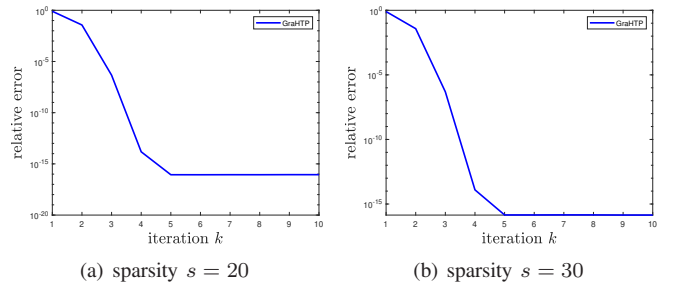


Fig. 9. Partial DFT sensing matrix: Relative error versus number of iterations for GraHTP, with fixed signal dimension $n = 2000$, sample size $m = 1500$.

IV. APPENDIX

A. Key Lemmas

In this subsection, we first give several key lemmas, which are essential for proving Theorem II.1, Theorem II.2 and Corollary II.1.

Lemma IV.1. *Let $\mathbf{a}_j, \mathbf{b}_j \in \mathbb{R}^n, j = 1, \dots, m$ be i.i.d. $\mathcal{N}(\mathbf{0}, \mathbf{I}_n/2)$ random vectors. For any sparse vector $\mathbf{z} \in \mathbb{R}^n$ independent from $\{\mathbf{a}_j, \mathbf{b}_j\}_{j=1}^m$ and for any subset $\mathcal{T} \subseteq [n]$ such that $\text{supp}(\mathbf{z}) \subseteq \mathcal{T}$ with $|\mathcal{T}| \leq t$ for some integer $t < n$, denote*

$$\Phi := \frac{1}{m} \sum_{j=1}^m |\mathbf{a}_{j,\mathcal{T}}^\top \mathbf{z}_\mathcal{T}|^2 \mathbf{a}_{j,\mathcal{T}} \mathbf{a}_{j,\mathcal{T}}^\top,$$

and

$$\Psi := \frac{1}{m} \sum_{j=1}^m (\mathbf{a}_{j,\mathcal{T}}^\top \mathbf{z}_\mathcal{T}) (\mathbf{b}_{j,\mathcal{T}}^\top \mathbf{z}_\mathcal{T}) \mathbf{a}_{j,\mathcal{T}} \mathbf{b}_{j,\mathcal{T}}^\top.$$

Then, for any $\delta \in (0, 1)$, with probability at least $1 - c_1 \delta^{-2} m^{-1} - m^{-4} - c_2 \exp(-c_3 \delta^2 m / \log m)$, it holds that

$$\|\Phi - (\|\mathbf{z}_\mathcal{T}\|_2^2 \mathbf{I}_{|\mathcal{T}|} + 2\mathbf{z}_\mathcal{T} \mathbf{z}_\mathcal{T}^\top)\|_2 \leq \frac{\delta}{16} \|\mathbf{z}\|_2^2, \quad (\text{IV.12})$$

and

$$\|\Psi - \mathbf{z}_\mathcal{T} \mathbf{z}_\mathcal{T}^\top\|_2 \leq \frac{\delta}{16} \|\mathbf{z}\|_2^2, \quad (\text{IV.13})$$

provided $m \geq C(\delta)t \log(n/t)$, where $C(\delta)$ is a constant depending on δ , and c_1, c_2 and c_3 are positive absolute constants.

Proof: The proof of this lemma is similar to that of Lemma A.3 in [37] and Lemma 6.3 in [46]. ■

The following lemma is an extension of Lemma V.5 in [24]. For the ease of notations, we denote

$$\begin{aligned} \mathbf{H}(\mathbf{z}) &:= \mathbf{J}(\mathbf{z})^\top \mathbf{J}(\mathbf{z}) \\ &= \frac{1}{m} \sum_{j=1}^m \left((\mathbf{a}_{jR}^\top \mathbf{z})^2 \mathbf{a}_{jR} \mathbf{a}_{jR}^\top + (\mathbf{a}_{jI}^\top \mathbf{z})^2 \mathbf{a}_{jI} \mathbf{a}_{jI}^\top \right. \\ &\quad \left. + (\mathbf{a}_{jR}^\top \mathbf{z})(\mathbf{a}_{jI}^\top \mathbf{z})(\mathbf{a}_{jI} \mathbf{a}_{jR}^\top + \mathbf{a}_{jR} \mathbf{a}_{jI}^\top) \right). \end{aligned} \quad (\text{IV.14})$$

Lemma IV.2. *Let $\mathbf{a}_j \in \mathbb{C}^n, j = 1, \dots, m$ be i.i.d. $\mathcal{CN}(\mathbf{0}, \mathbf{I}_n)$ Gaussian random vectors. For any sparse vector $\mathbf{z} \in \mathbb{R}^n$ and subset $\mathcal{T} \subseteq [n]$ such that $\text{supp}(\mathbf{z}) \subseteq \mathcal{T}$ with $|\mathcal{T}| \leq t$ for some integer $t < n$, under the event (IV.12) and (IV.13), we have*

$$\left(\frac{1}{2} - \frac{\delta}{4}\right) \|\mathbf{z}\|_2^2 \leq \|\mathbf{H}_{\mathcal{T},\mathcal{T}}(\mathbf{z})\|_2 \leq \left(2 + \frac{\delta}{4}\right) \|\mathbf{z}\|_2^2, \quad (\text{IV.15})$$

and $\mathbf{H}_{\mathcal{T},\mathcal{T}}(\mathbf{z})$ is invertible and

$$\|(\mathbf{H}_{\mathcal{T},\mathcal{T}}(\mathbf{z}))^{-1}\|_2 \leq \frac{4}{(2 - \delta) \|\mathbf{z}\|_2^2}. \quad (\text{IV.16})$$

Proof: Note that $\text{supp}(\mathbf{z}) \subseteq \mathcal{T}$, which implies that $\mathbf{a}_{jR}^\top \mathbf{z} = \mathbf{a}_{jR,\mathcal{T}}^\top \mathbf{z}_\mathcal{T}$ and $\mathbf{a}_{jI}^\top \mathbf{z} = \mathbf{a}_{jI,\mathcal{T}}^\top \mathbf{z}_\mathcal{T}$, then according to (IV.14) we have

$$\begin{aligned} &\mathbf{H}_{\mathcal{T},\mathcal{T}}(\mathbf{z}) \\ &= \frac{1}{m} \sum_{j=1}^m \left((\mathbf{a}_{jR,\mathcal{T}}^\top \mathbf{z}_\mathcal{T})^2 \mathbf{a}_{jR,\mathcal{T}} \mathbf{a}_{jR,\mathcal{T}}^\top + (\mathbf{a}_{jI,\mathcal{T}}^\top \mathbf{z}_\mathcal{T})^2 \mathbf{a}_{jI,\mathcal{T}} \mathbf{a}_{jI,\mathcal{T}}^\top \right. \\ &\quad \left. + (\mathbf{a}_{jR,\mathcal{T}}^\top \mathbf{z}_\mathcal{T})(\mathbf{a}_{jI,\mathcal{T}}^\top \mathbf{z}_\mathcal{T})(\mathbf{a}_{jI,\mathcal{T}} \mathbf{a}_{jR,\mathcal{T}}^\top + \mathbf{a}_{jR,\mathcal{T}} \mathbf{a}_{jI,\mathcal{T}}^\top) \right). \end{aligned}$$

Assuming event (IV.12) and (IV.13) holds. By direct calculation, we have

$$\mathbb{E}(\mathbf{H}_{\mathcal{T},\mathcal{T}}(\mathbf{z})) = \frac{1}{2} (\|\mathbf{z}\|_2^2 \mathbf{I}_{|\mathcal{T}|} + 3\mathbf{z}_\mathcal{T} \mathbf{z}_\mathcal{T}^\top),$$

and the minimum and maximum eigenvalues of $\mathbb{E}(\mathbf{H}_{\mathcal{T},\mathcal{T}}(\mathbf{z}))$

$$\lambda_{\min}(\mathbb{E}(\mathbf{H}_{\mathcal{T},\mathcal{T}}(\mathbf{z}))) = \frac{1}{2} \|\mathbf{z}\|_2^2, \quad (\text{IV.17})$$

$$\lambda_{\max}(\mathbb{E}(\mathbf{H}_{\mathcal{T},\mathcal{T}}(\mathbf{z}))) = 2 \|\mathbf{z}\|_2^2. \quad (\text{IV.18})$$

Then by Lemma IV.1 we have

$$\begin{aligned} &\|\mathbf{H}_{\mathcal{T},\mathcal{T}}(\mathbf{z}) - \mathbb{E}(\mathbf{H}_{\mathcal{T},\mathcal{T}}(\mathbf{z}))\|_2 \\ &\leq 2 \left\| \frac{1}{m} \sum_{j=1}^m (\mathbf{a}_{jR,\mathcal{T}}^\top \mathbf{z}_\mathcal{T})^2 \mathbf{a}_{jR,\mathcal{T}} \mathbf{a}_{jR,\mathcal{T}}^\top - \frac{1}{4} (\|\mathbf{z}\|_2^2 \mathbf{I}_{|\mathcal{T}|} + 2\mathbf{z}_\mathcal{T} \mathbf{z}_\mathcal{T}^\top) \right\|_2 \\ &\quad + 2 \left\| \frac{1}{m} \sum_{j=1}^m (\mathbf{a}_{jR,\mathcal{T}}^\top \mathbf{z}_\mathcal{T})(\mathbf{a}_{jI,\mathcal{T}}^\top \mathbf{z}_\mathcal{T}) \mathbf{a}_{jI,\mathcal{T}} \mathbf{a}_{jR,\mathcal{T}}^\top - \frac{1}{4} \mathbf{z}_\mathcal{T} \mathbf{z}_\mathcal{T}^\top \right\|_2 \\ &\leq \frac{\delta}{4} \|\mathbf{z}\|_2^2, \end{aligned}$$

thus, by Weyl's inequality we obtain

$$|\lambda_{\max}(\mathbf{H}_{\mathcal{T},\mathcal{T}}(\mathbf{z})) - \lambda_{\max}(\mathbb{E}(\mathbf{H}_{\mathcal{T},\mathcal{T}}(\mathbf{z})))| \leq \frac{\delta}{4} \|\mathbf{z}\|_2^2,$$

$$|\lambda_{\min}(\mathbf{H}_{\mathcal{T},\mathcal{T}}(\mathbf{z})) - \lambda_{\min}(\mathbb{E}(\mathbf{H}_{\mathcal{T},\mathcal{T}}(\mathbf{z})))| \leq \frac{\delta}{4} \|\mathbf{z}\|_2^2.$$

Together with (IV.17) and (IV.18), we have

$$\begin{aligned} \left(\frac{1}{2} - \frac{\delta}{4}\right) \|\mathbf{z}\|_2^2 &\leq \lambda_{\min}(\mathbf{H}_{\mathcal{T},\mathcal{T}}(\mathbf{z})) \\ &\leq \lambda_{\max}(\mathbf{H}_{\mathcal{T},\mathcal{T}}(\mathbf{z})) \leq \left(2 + \frac{\delta}{4}\right) \|\mathbf{z}\|_2^2, \end{aligned}$$

and

$$\lambda_{\max}((\mathbf{H}_{\mathcal{T},\mathcal{T}}(\mathbf{z}))^{-1}) = 1/\lambda_{\min}(\mathbf{H}_{\mathcal{T},\mathcal{T}}(\mathbf{z})) \leq \frac{4}{(2 - \delta) \|\mathbf{z}\|_2^2},$$

which completes the proof. ■

Lemma IV.3. *Let $\mathbf{a}_j \in \mathbb{C}^n, j = 1, \dots, m$ be i.i.d. $\mathcal{CN}(\mathbf{0}, \mathbf{I}_n)$ Gaussian random vectors. For any sparse vector $\mathbf{z} \in \mathbb{R}^n$ and subsets $\mathcal{S}, \mathcal{T} \subseteq [n]$ satisfying $\mathcal{S} \subseteq \mathcal{T}$ with $|\mathcal{T}| \leq t$ for some integer $t < n$, under the event (IV.12) and (IV.13) with $\text{supp}(\mathbf{z}) \subseteq \mathcal{S}$, it holds that*

$$\|\mathbf{H}_{\mathcal{S},\mathcal{T} \setminus \mathcal{S}}(\mathbf{z})\|_2 \leq \frac{\delta}{4} \|\mathbf{z}\|_2^2.$$

Proof: Note that \mathcal{S} and $\mathcal{T} \setminus \mathcal{S}$ are two disjoint subsets of \mathcal{T} , and we have

$$\mathbb{E}[\mathbf{H}_{\mathcal{S},\mathcal{T} \setminus \mathcal{S}}(\mathbf{z})] = \mathbf{z}_\mathcal{S} \mathbf{z}_{\mathcal{T} \setminus \mathcal{S}}^\top = \mathbf{0},$$

thus $\mathbf{H}_{\mathcal{S}, \mathcal{T} \setminus \mathcal{S}}(\mathbf{z})$ is a sub-matrix of $\mathbf{H}_{\mathcal{T}, \mathcal{T}}(\mathbf{z}) - \mathbb{E}(\mathbf{H}_{\mathcal{T}, \mathcal{T}}(\mathbf{z}))$. According to Lemma IV.2 we then have

$$\|\mathbf{H}_{\mathcal{S}, \mathcal{T} \setminus \mathcal{S}}(\mathbf{z})\|_2 \leq \|\mathbf{H}_{\mathcal{T}, \mathcal{T}}(\mathbf{z}) - \mathbb{E}(\mathbf{H}_{\mathcal{T}, \mathcal{T}}(\mathbf{z}))\|_2 \leq \frac{\delta}{4} \|\mathbf{z}\|_2^2,$$

which completes the proof. \blacksquare

Lemma IV.4. For any sparse vector \mathbf{z} , $\mathbf{x} \in \mathbb{R}^n$ and any subset $\mathcal{T} \subseteq [n]$ that satisfies $\text{supp}(\mathbf{z}) \subseteq \mathcal{T}$, $\text{supp}(\mathbf{x}) \subseteq \mathcal{T}$ with $|\mathcal{T}| \leq t$ for some integer $t < n$. Let $\mathbf{a}_j \in \mathbb{C}^n$, $j = 1, \dots, m$ be i.i.d. $\mathcal{CN}(0, \mathbf{I}_n)$ Gaussian random vectors independent with \mathbf{z} and \mathbf{x} . Set $\mathbf{h} := \mathbf{z} - \mathbf{x}$, then under the event (IV.12) and (IV.13), it holds

$$\|\mathbf{J}_{\mathcal{T}}(\mathbf{h})^\top \mathbf{J}_{\mathcal{T}}(\mathbf{h})\|_2 \leq (2 + \delta) \|\mathbf{z} - \mathbf{x}\|_2^2. \quad (\text{IV.19})$$

Proof: Since $\{\mathbf{a}_j\}_{j=1}^m$ are vectors rotationally invariant and independent with \mathbf{z} and \mathbf{x} , it is enough for us to consider that $\mathbf{x} = \|\mathbf{x}\|_2 \mathbf{e}_1$ and $\mathbf{z} = \|\mathbf{z}\|_2 (\omega \mathbf{e}_1 + \sqrt{1 - \omega^2} \mathbf{e}_2)$, where ω is a positive real number obeying $\omega \in (0, 1)$. For simplicity, we use \mathbf{d}_j and \mathbf{g}_j to denote $\mathbf{a}_{jR, \mathcal{T}}$ and $\mathbf{a}_{jI, \mathcal{T}}$ respectively for $j = 1, \dots, m$. Then we have

$$\begin{aligned} & \|\mathbf{J}_{\mathcal{T}}(\mathbf{h})^\top \mathbf{J}_{\mathcal{T}}(\mathbf{h})\|_2 \\ &= \left\| \frac{1}{m} \sum_{j=1}^{2m} \left((\mathbf{d}_j^\top (\mathbf{z}_{\mathcal{T}} - \mathbf{x}_{\mathcal{T}}))^2 \mathbf{d}_j \mathbf{d}_j^\top + (\mathbf{g}_j^\top (\mathbf{z}_{\mathcal{T}} - \mathbf{x}_{\mathcal{T}}))^2 \mathbf{g}_j \mathbf{g}_j^\top \right. \right. \\ & \quad \left. \left. + (\mathbf{d}_j^\top (\mathbf{z}_{\mathcal{T}} - \mathbf{x}_{\mathcal{T}})) (\mathbf{g}_j^\top (\mathbf{z}_{\mathcal{T}} - \mathbf{x}_{\mathcal{T}})) (\mathbf{d}_j \mathbf{g}_j^\top + \mathbf{g}_j \mathbf{d}_j^\top) \right) \right\|_2 \\ &= \|\mathbf{z}_{\mathcal{T}} - \mathbf{x}_{\mathcal{T}}\|_2^2 \|\mathbf{G}\|_2, \end{aligned} \quad (\text{IV.20})$$

where

$$\mathbf{G} := \frac{1}{m} \sum_{j=1}^m (\kappa_{1j}^2 \mathbf{d}_j \mathbf{d}_j^\top + \kappa_{2j}^2 \mathbf{g}_j \mathbf{g}_j^\top + \kappa_{1j} \kappa_{2j} (\mathbf{d}_j \mathbf{g}_j^\top + \mathbf{g}_j \mathbf{d}_j^\top)),$$

and $\kappa_{1j} := \mathbf{d}_j^\top (t_1 \mathbf{e}_{1, \mathcal{T}} + t_2 \mathbf{e}_{2, \mathcal{T}})$, $\kappa_{2j} := \mathbf{g}_j^\top (t_1 \mathbf{e}_{1, \mathcal{T}} + t_2 \mathbf{e}_{2, \mathcal{T}})$, $t_1 = \frac{\omega \|\mathbf{z}_{\mathcal{T}}\|_2 - \|\mathbf{x}_{\mathcal{T}}^\dagger\|_2}{\|\mathbf{z}_{\mathcal{T}} - \mathbf{x}_{\mathcal{T}}\|_2}$, $t_2 = \frac{\sqrt{1 - \omega^2} \|\mathbf{z}_{\mathcal{T}}\|_2}{\|\mathbf{z}_{\mathcal{T}} - \mathbf{x}_{\mathcal{T}}\|_2}$ and $t_1^2 + t_2^2 = 1$. According to Lemma IV.2, we obtain

$$\|\mathbf{G}\|_2 \leq 2 + \frac{\delta}{4},$$

which leads to

$$\|\mathbf{J}_{\mathcal{T}}(\mathbf{h})^\top \mathbf{J}_{\mathcal{T}}(\mathbf{h})\|_2 \leq (2 + \frac{\delta}{4}) \|\mathbf{z} - \mathbf{x}\|_2^2.$$

This completes the proof. \blacksquare

The following Lemma provides an upper bound for hard thresholding.

Lemma IV.5. For any sparse vector $\mathbf{x} \in \mathbb{R}^n$ satisfying $\|\mathbf{x}\|_0 \leq s$ and any vector $\mathbf{v} \in \mathbb{R}^n$, define $\mathbf{u} := \mathcal{H}_s(\mathbf{v})$, $\mathcal{S}_u := \text{supp}(\mathbf{u})$ and $\mathcal{S} := \text{supp}(\mathbf{x})$, then we have the following inequality:

$$\|\mathbf{u} - \mathbf{x}\|_2^2 \leq \frac{3 + \sqrt{5}}{2} \|\mathbf{v}_{\mathcal{S}_u \cup \mathcal{S}} - \mathbf{x}_{\mathcal{S}_u \cup \mathcal{S}}\|_2^2.$$

Proof: The proof of this lemma is a direct application of Theorem 1 in [47] since $n \geq 2s$. \blacksquare

Now we proceed to give the proof of Theorem II.1, and we only consider the case where $\|\mathbf{z}^0 - \mathbf{x}^\dagger\|_2 \leq \|\mathbf{z}^0 + \mathbf{x}^\dagger\|_2$ since the case where $\|\mathbf{z}^0 + \mathbf{x}^\dagger\|_2 \leq \|\mathbf{z}^0 - \mathbf{x}^\dagger\|_2$ can be proved in a similar way.

B. Proof of Part a.) of Theorem II.1

We first give the proof of part a.) of Theorem II.1, which gives an upper bound on the estimation error of the vector obtained by applying the hard thresholding operator to the output of gradient descent.

Proof: For any fixed \mathbf{z}^k satisfying $\|\mathbf{z}^k\|_0 \leq s$ and $\mathbf{z}^k \in \mathcal{E}(\delta)$, denote $\mathcal{S}^\dagger := \text{supp}(\mathbf{x}^\dagger)$, $\mathcal{S}_k := \text{supp}(\mathbf{z}^k)$, $\mathcal{S}_{k+1} := \text{supp}(\mathbf{u}^k)$, $\mathcal{T}_{k+1} := \mathcal{S}_k \cup \mathcal{S}_{k+1} \cup \mathcal{S}^\dagger$, $\mathbf{h}^k := \mathbf{z}^k - \mathbf{x}^\dagger$ and

$$\mathbf{v}^k := \mathbf{z}^k - \mu^k \nabla f(\mathbf{z}^k),$$

Then $\mathbf{u}^k = \mathcal{H}_s(\mathbf{v}^k)$. According to the definition of \mathcal{T}_{k+1} , the size of \mathcal{T}_{k+1} is at most $3s$, i.e., $|\mathcal{T}_{k+1}| \leq 3s$. This proof is under event (IV.12) with $\mathbf{z} = \mathbf{z}^k$ and $\mathcal{T} = \mathcal{T}_{k+1}$. Noting that \mathbf{u}^k is the best s -term approximation of \mathbf{v}^k , then by Lemma IV.5 and $\mathcal{S}_{k+1} \cup \mathcal{S}^\dagger \subseteq \mathcal{T}_{k+1}$, we obtain

$$\begin{aligned} \|\mathbf{u}^k - \mathbf{x}^\dagger\|_2 &= \|\mathbf{u}_{\mathcal{S}_{k+1} \cup \mathcal{S}^\dagger}^k - \mathbf{x}_{\mathcal{S}_{k+1} \cup \mathcal{S}^\dagger}^\dagger\|_2 \\ &\leq \sqrt{\frac{3 + \sqrt{5}}{2}} \|\mathbf{v}_{\mathcal{T}_{k+1}}^k - \mathbf{x}_{\mathcal{T}_{k+1}}^\dagger\|_2. \end{aligned} \quad (\text{IV.21})$$

Since $\mathcal{S}_k, \mathcal{S}^\dagger \subseteq \mathcal{T}_{k+1}$, it holds that

$$\begin{aligned} & \nabla f_{\mathcal{T}_{k+1}}(\mathbf{z}^k) \\ &= \frac{1}{m} \sum_{j=1}^m \left((\mathbf{a}_{jR}^\top \mathbf{z}^k)^2 + (\mathbf{a}_{jI}^\top \mathbf{z}^k)^2 - (\mathbf{a}_{jR}^\top \mathbf{x}^\dagger)^2 - (\mathbf{a}_{jI}^\top \mathbf{x}^\dagger)^2 \right) \\ & \quad \cdot (\mathbf{a}_{jR, \mathcal{T}_{k+1}} \mathbf{a}_{jR}^\top \mathbf{z}^k + \mathbf{a}_{jI, \mathcal{T}_{k+1}} \mathbf{a}_{jI}^\top \mathbf{z}^k) \\ &= \mathbf{J}_{\mathcal{T}_{k+1}}(\mathbf{z}^k)^\top \left(\mathbf{J}_{\mathcal{T}_{k+1}}(\mathbf{z}^k) + \mathbf{J}_{\mathcal{T}_{k+1}}(\mathbf{x}^\dagger) \right) (\mathbf{z}_{\mathcal{T}_{k+1}}^k - \mathbf{x}_{\mathcal{T}_{k+1}}^\dagger) \\ &= 2\mathbf{H}_{\mathcal{T}_{k+1}, \mathcal{T}_{k+1}}(\mathbf{z}^k) \mathbf{h}_{\mathcal{T}_{k+1}}^k - \mathbf{J}_{\mathcal{T}_{k+1}}(\mathbf{z}^k)^\top \mathbf{J}_{\mathcal{T}_{k+1}}(\mathbf{h}^k) \mathbf{h}_{\mathcal{T}_{k+1}}^k. \end{aligned}$$

According to the definition of \mathbf{v}^k , a simple calculation gives

$$\begin{aligned} \|\mathbf{v}_{\mathcal{T}_{k+1}}^k - \mathbf{x}_{\mathcal{T}_{k+1}}^\dagger\|_2 &= \left\| \mathbf{z}_{\mathcal{T}_{k+1}}^k - \mathbf{x}_{\mathcal{T}_{k+1}}^\dagger - \mu^k \nabla f_{\mathcal{T}_{k+1}}(\mathbf{z}^k) \right\|_2 \\ &\leq \underbrace{\left\| (\mathbf{I} - 2\mu^k \mathbf{H}_{\mathcal{T}_{k+1}, \mathcal{T}_{k+1}}(\mathbf{z}^k)) \mathbf{h}_{\mathcal{T}_{k+1}}^k \right\|_2}_{I_1} \\ & \quad + \underbrace{\mu^k \left\| \mathbf{J}_{\mathcal{T}_{k+1}}(\mathbf{z}^k)^\top \mathbf{J}_{\mathcal{T}_{k+1}}(\mathbf{h}^k) \mathbf{h}_{\mathcal{T}_{k+1}}^k \right\|_2}_{I_2}. \end{aligned}$$

Next we will estimate I_1 and I_2 sequentially. Since $\|\mathbf{h}^k\|_2 = \|\mathbf{z}^k - \mathbf{x}^\dagger\|_2 \leq \delta \|\mathbf{x}^\dagger\|_2$, we obtain

$$(1 - \delta) \|\mathbf{x}^\dagger\|_2 \leq \|\mathbf{z}^k\|_2 \leq (1 + \delta) \|\mathbf{x}^\dagger\|_2.$$

For I_1 : Let $\mu^k \in \left(\frac{1 - \sqrt{\frac{2}{3 + \sqrt{5}}}}{(1 - \frac{9\delta}{2} - \frac{\delta^2}{4} - \frac{3\delta^3}{4}) \|\mathbf{x}^\dagger\|_2^2}, \frac{2}{(5 + 6\delta + 7\delta^2) \|\mathbf{x}^\dagger\|_2^2} \right)$. By Lemma IV.2 with $\mathbf{z} = \mathbf{z}^k$ and $\mathcal{T} = \mathcal{T}_{k+1}$, we have

$$\begin{aligned} \lambda_{\min}(\mathbf{H}_{\mathcal{T}_{k+1}, \mathcal{T}_{k+1}}(\mathbf{z}^k)) &\geq \left(\frac{1}{2} - \frac{\delta}{4} \right) (1 - \delta)^2 \|\mathbf{x}^\dagger\|_2^2 \\ \lambda_{\max}(\mathbf{H}_{\mathcal{T}_{k+1}, \mathcal{T}_{k+1}}(\mathbf{z}^k)) &\leq \left(2 + \frac{\delta}{4} \right) (1 + \delta)^2 \|\mathbf{x}^\dagger\|_2^2. \end{aligned} \quad (\text{IV.22})$$

According to Weyl's inequality, we have

$$\|\mathbf{I} - 2\mu^k \mathbf{H}_{\mathcal{T}_{k+1}, \mathcal{T}_{k+1}}(\mathbf{z}^k)\|_2 \leq l_0,$$

where $l_0 = 1 - \mu^k \|\mathbf{x}^\dagger\|_2^2 (1 - \frac{\delta}{2})(1 - \delta)^2$. Thus

$$I_1 \leq l_0 \left\| \mathbf{z}_{\mathcal{T}_{k+1}}^k - \mathbf{x}_{\mathcal{T}_{k+1}}^\dagger \right\|_2.$$

For I_2 : An application of Lemma IV.4 with $\mathbf{h} = \mathbf{h}^k$ and $\mathcal{T} = \mathcal{T}_{k+1}$ implies

$$\left\| \mathbf{J}_{\mathcal{T}_{k+1}}(\mathbf{h}^k) \right\|_2 \leq \delta \sqrt{2 + \frac{\delta}{4}} \|\mathbf{x}^\dagger\|_2,$$

together with (IV.22) we obtain

$$I_2 \leq \mu^k \|\mathbf{x}^\dagger\|_2^2 (2 + \frac{\delta}{4}) \delta (1 + \delta) \left\| \mathbf{z}_{\mathcal{T}_{k+1}}^k - \mathbf{x}_{\mathcal{T}_{k+1}}^\dagger \right\|_2.$$

Combining all pieces together, we have

$$\left\| \mathbf{v}_{\mathcal{T}_{k+1}}^k - \mathbf{x}_{\mathcal{T}_{k+1}}^\dagger \right\|_2 \leq I_1 + I_2 \leq \rho_0 \left\| \mathbf{z}_{\mathcal{T}_{k+1}}^k - \mathbf{x}_{\mathcal{T}_{k+1}}^\dagger \right\|_2,$$

where $\rho_0 = 1 - \mu^k \|\mathbf{x}^\dagger\|_2^2 (1 - \frac{9\delta}{2} - \frac{\delta^2}{4} - \frac{3\delta^3}{4})$. By (IV.21) we then have

$$\|\mathbf{u}^k - \mathbf{x}^\dagger\|_2 \leq \rho \|\mathbf{z}^k - \mathbf{x}^\dagger\|_2,$$

where $\rho = \sqrt{\frac{3+\sqrt{5}}{2}} (1 - \mu^k \|\mathbf{x}^\dagger\|_2^2 (1 - \frac{9\delta}{2} - \frac{\delta^2}{4} - \frac{3\delta^3}{4}))$.

For $\mu^k \in \left(\frac{1 - \sqrt{\frac{2}{3+\sqrt{5}}}}{(1 - \frac{9\delta}{2} - \frac{\delta^2}{4} - \frac{3\delta^3}{4}) \|\mathbf{x}^\dagger\|_2^2}, \frac{2}{(5+6\delta+7\delta^2) \|\mathbf{x}^\dagger\|_2^2} \right)$ and $\delta \in (0, 0.008)$, we have $\rho \in (0, 1)$, which completes the proof. ■

C. Proof of Part b.) of Theorem II.1

Next thing we concern about is the relationship between the estimation error of vectors $\mathbf{z}^{k,0}$ and \mathbf{z}^{k+1} obtained by Algorithm 1. We now give the proof of first phase.

Proof: Given a vector \mathbf{z}^k satisfying $\mathbf{z}^k \in \mathcal{E}(\delta)$ and a vector \mathbf{u}^k satisfying $\|\mathbf{u}^k - \mathbf{x}^\dagger\| \leq \rho \|\mathbf{z}^k - \mathbf{x}^\dagger\|$ where $\rho \in (0, 1)$, $\|\mathbf{u}^k\|_0 \leq s$ and $\mathcal{S}_{k+1} = \text{supp}(\mathbf{u}^k)$. Suppose that $\|\mathbf{z}^{k,0} - \mathbf{x}^\dagger\| \leq \|\mathbf{u}^k - \mathbf{x}^\dagger\|$ and $\text{supp}(\mathbf{z}^{k,0}) = \mathcal{S}_{k+1}$. Denote $\mathbf{h}^{k,0} := \mathbf{z}^{k,0} - \mathbf{x}^\dagger$, $\mathcal{S}^\dagger := \text{supp}(\mathbf{x}^\dagger)$, $\mathcal{S}_k := \text{supp}(\mathbf{z}^k)$ and $\mathcal{T}_{k+1} := \mathcal{S}_k \cup \mathcal{S}_{k+1} \cup \mathcal{S}^\dagger$, which implies $|\mathcal{T}_{k+1}| \leq 3s$. The proof is under event (IV.12) and (IV.13). First we have

$$\begin{aligned} & \mathbf{J}_{\mathcal{S}_{k+1}}(\mathbf{z}^{k,0})^\top \mathbf{F}(\mathbf{z}^{k,0}) \\ &= \frac{1}{2m} \sum_{j=1}^m \left((\mathbf{a}_{jR}^\top \mathbf{z}^{k,0})^2 + (\mathbf{a}_{jI}^\top \mathbf{z}^{k,0})^2 - (\mathbf{a}_{jR}^\top \mathbf{x}^\dagger)^2 - (\mathbf{a}_{jI}^\top \mathbf{x}^\dagger)^2 \right) \\ & \quad \cdot (\mathbf{a}_{jR, \mathcal{S}_{k+1}} \mathbf{a}_{jR}^\top \mathbf{z}^{k,0} + \mathbf{a}_{jI, \mathcal{S}_{k+1}} \mathbf{a}_{jI}^\top \mathbf{z}^{k,0}) \\ &= \mathbf{H}_{\mathcal{S}_{k+1}, \mathcal{T}_{k+1}}(\mathbf{z}^{k,0}) \mathbf{h}_{\mathcal{T}_{k+1}}^{k,0} - \frac{1}{2} \mathbf{J}_{\mathcal{S}_{k+1}}(\mathbf{z}^{k,0})^\top \mathbf{J}_{\mathcal{T}_{k+1}}(\mathbf{h}^{k,0}) \mathbf{h}_{\mathcal{T}_{k+1}}^{k,0}. \end{aligned} \quad (\text{IV.23})$$

Since $\|\mathbf{h}^{k,0}\|_2 = \|\mathbf{z}^{k,0} - \mathbf{x}^\dagger\|_2 \leq \rho \delta \|\mathbf{x}^\dagger\|_2$, we have

$$(1 - \rho\delta) \|\mathbf{x}^\dagger\|_2 \leq \|\mathbf{z}^{k,0}\|_2 \leq (1 + \rho\delta) \|\mathbf{x}^\dagger\|_2.$$

By Lemma IV.2 with $\mathbf{z} = \mathbf{z}^{k,0}$ and $\mathcal{T} = \mathcal{T}_{k+1}$, we obtain

$$\left\| (\mathbf{H}_{\mathcal{S}_{k+1}, \mathcal{S}_{k+1}}(\mathbf{z}^{k,0}))^{-1} \right\|_2 \leq \frac{4}{(2 - \delta)(1 - \rho\delta)^2 \|\mathbf{x}^\dagger\|_2^2}, \quad (\text{IV.24})$$

and

$$\begin{aligned} & \left\| (\mathbf{H}_{\mathcal{S}_{k+1}, \mathcal{S}_{k+1}}(\mathbf{z}^{k,0}))^{-1} \mathbf{J}_{\mathcal{S}_{k+1}}(\mathbf{z}^{k,0})^\top \right\|_2 \\ & \leq \frac{2}{\sqrt{2 - \delta}(1 - \rho\delta) \|\mathbf{x}^\dagger\|_2}. \end{aligned} \quad (\text{IV.25})$$

By Lemma IV.3 with $\mathbf{z} = \mathbf{z}^{k,0}$ and $\mathcal{T} = \mathcal{T}_{k+1}$ we have

$$\left\| \mathbf{H}_{\mathcal{S}_{k+1}, \mathcal{T}_{k+1} \setminus \mathcal{S}_{k+1}}(\mathbf{z}^{k,0}) \right\|_2 \leq \frac{\delta}{4} (1 + \rho\delta)^2 \|\mathbf{x}^\dagger\|_2^2. \quad (\text{IV.26})$$

According to Lemma IV.4 with $\mathbf{h} = \mathbf{h}^{k,0}$ and $\mathcal{T} = \mathcal{T}_{k+1}$, then

$$\left\| \mathbf{J}_{\mathcal{T}_{k+1}}(\mathbf{h}^{k,0}) \right\|_2 \leq \sqrt{2 + \frac{\delta}{4}} \rho \delta \|\mathbf{x}^\dagger\|_2. \quad (\text{IV.27})$$

We now decompose the term $\|\mathbf{z}^{k+1} - \mathbf{x}^\dagger\|_2$ into two parts and bound them respectively:

$$\begin{aligned} & \left\| \mathbf{z}^{k+1} - \mathbf{x}^\dagger \right\|_2^2 \\ &= \left\| \mathbf{z}_{\mathcal{S}^\dagger \setminus \mathcal{S}_{k+1}}^{k+1} - \mathbf{x}_{\mathcal{S}^\dagger \setminus \mathcal{S}_{k+1}}^\dagger \right\|_2^2 + \left\| \mathbf{z}_{\mathcal{S}_{k+1}}^{k+1} - \mathbf{x}_{\mathcal{S}_{k+1}}^\dagger \right\|_2^2 \\ &= \left\| \mathbf{x}_{\mathcal{S}^\dagger \setminus \mathcal{S}_{k+1}}^\dagger \right\|_2^2 + \left\| \mathbf{z}_{\mathcal{S}_{k+1}}^{k+1} - \mathbf{x}_{\mathcal{S}_{k+1}}^\dagger \right\|_2^2. \end{aligned}$$

Note that $\mathbf{x}_{\mathcal{S}^\dagger \setminus \mathcal{S}_{k+1}}^\dagger$ is a subvector of $\mathbf{z}^{k,0} - \mathbf{x}^\dagger$, then we have

$$\left\| \mathbf{x}_{\mathcal{S}^\dagger \setminus \mathcal{S}_{k+1}}^\dagger \right\|_2 \leq \|\mathbf{z}^{k,0} - \mathbf{x}^\dagger\|_2.$$

According to update rule (II.10) for $L = 1$ and (IV.23) we have

$$\begin{aligned} & \mathbf{H}_{\mathcal{S}_{k+1}, \mathcal{S}_{k+1}}(\mathbf{z}^{k,0}) (\mathbf{z}_{\mathcal{S}_{k+1}}^{k+1} - \mathbf{x}_{\mathcal{S}_{k+1}}^\dagger) \\ &= \mathbf{H}_{\mathcal{S}_{k+1}, \mathcal{S}_{k+1}}(\mathbf{z}^{k,0}) (\mathbf{z}_{\mathcal{S}_{k+1}}^{k,0} - \mathbf{x}_{\mathcal{S}_{k+1}}^\dagger) - \mathbf{J}_{\mathcal{S}_{k+1}}(\mathbf{z}^{k,0})^\top \mathbf{F}(\mathbf{z}^{k,0}) \\ &= \frac{1}{2} \mathbf{J}_{\mathcal{S}_{k+1}}(\mathbf{z}^{k,0})^\top \mathbf{J}_{\mathcal{T}_{k+1}}(\mathbf{h}^{k,0}) \mathbf{h}_{\mathcal{T}_{k+1}}^{k,0} \\ & \quad - \mathbf{H}_{\mathcal{S}_{k+1}, \mathcal{T}_{k+1} \setminus \mathcal{S}_{k+1}}(\mathbf{z}^{k,0}) \mathbf{h}_{\mathcal{T}_{k+1} \setminus \mathcal{S}_{k+1}}^{k,0}, \end{aligned} \quad (\text{IV.28})$$

thus

$$\begin{aligned} & \left\| \mathbf{z}_{\mathcal{S}_{k+1}}^{k+1} - \mathbf{x}_{\mathcal{S}_{k+1}}^\dagger \right\|_2 \\ &= \left\| (\mathbf{H}_{\mathcal{S}_{k+1}, \mathcal{S}_{k+1}}(\mathbf{z}^{k,0}))^{-1} \mathbf{H}_{\mathcal{S}_{k+1}, \mathcal{S}_{k+1}}(\mathbf{z}^{k,0}) (\mathbf{z}_{\mathcal{S}_{k+1}}^{k+1} - \mathbf{x}_{\mathcal{S}_{k+1}}^\dagger) \right\|_2 \\ &\leq \frac{1}{2} \left\| (\mathbf{H}_{\mathcal{S}_{k+1}, \mathcal{S}_{k+1}}(\mathbf{z}^{k,0}))^{-1} \mathbf{J}_{\mathcal{S}_{k+1}}(\mathbf{z}^{k,0})^\top \mathbf{J}_{\mathcal{T}_{k+1}}(\mathbf{h}^{k,0}) \mathbf{h}_{\mathcal{T}_{k+1}}^{k,0} \right\|_2 \\ & \quad + \left\| (\mathbf{H}_{\mathcal{S}_{k+1}, \mathcal{S}_{k+1}}(\mathbf{z}^{k,0}))^{-1} \mathbf{H}_{\mathcal{S}_{k+1}, \mathcal{T}_{k+1} \setminus \mathcal{S}_{k+1}}(\mathbf{z}^{k,0}) \mathbf{h}_{\mathcal{T}_{k+1} \setminus \mathcal{S}_{k+1}}^{k,0} \right\|_2, \end{aligned}$$

together with (IV.24), (IV.25), (IV.26) and (IV.27) yields that

$$\begin{aligned} & \left\| \mathbf{z}_{\mathcal{S}_{k+1}}^{k+1} - \mathbf{x}_{\mathcal{S}_{k+1}}^\dagger \right\|_2 \\ &\leq \frac{\sqrt{8 + \delta} \rho \delta}{2\sqrt{2 - \delta}(1 - \rho\delta)} \left\| \mathbf{z}_{\mathcal{T}_{k+1}}^{k,0} - \mathbf{x}_{\mathcal{T}_{k+1}}^\dagger \right\|_2 \\ & \quad + \frac{\delta(1 + \rho\delta)^2}{(2 - \delta)(1 - \rho\delta)^2} \left\| \mathbf{z}_{\mathcal{T}_{k+1} \setminus \mathcal{S}_{k+1}}^{k,0} - \mathbf{x}_{\mathcal{T}_{k+1} \setminus \mathcal{S}_{k+1}}^\dagger \right\|_2 \\ &\leq \alpha_0 \|\mathbf{z}^{k,0} - \mathbf{x}^\dagger\|_2, \end{aligned}$$

where $\alpha_0 = \frac{\sqrt{(2 - \delta)(8 + \delta)} \rho \delta (1 - \rho\delta) + 2\delta(1 + \rho\delta)^2}{2(2 - \delta)(1 - \rho\delta)^2}$. Combining all the terms together, we obtain

$$\begin{aligned} \left\| \mathbf{z}^{k+1} - \mathbf{x}^\dagger \right\|_2 &= \sqrt{\left\| \mathbf{z}_{\mathcal{S}_{k+1}^c}^{k+1} - \mathbf{x}_{\mathcal{S}_{k+1}^c}^\dagger \right\|_2^2 + \left\| \mathbf{z}_{\mathcal{S}_{k+1}}^{k+1} - \mathbf{x}_{\mathcal{S}_{k+1}}^\dagger \right\|_2^2} \\ &\leq \sqrt{\alpha_0^2 + 1} \|\mathbf{z}^{k,0} - \mathbf{x}^\dagger\|_2 \\ &\leq \rho \sqrt{\alpha_0^2 + 1} \|\mathbf{z}^k - \mathbf{x}^\dagger\|_2. \end{aligned}$$

Let $\alpha := \rho \sqrt{\alpha_0^2 + 1}$. We can choose parameters δ and μ^k to make sure that $\alpha \in (0, 1)$. For example, we can set

$\mu^k \in (0.3910/\|\mathbf{x}^\dagger\|_2^2, 0.3975/\|\mathbf{x}^\dagger\|_2^2)$, such that $\alpha \in (0, 1)$ if provided $\delta \leq 0.005$. Therefore, we have $\|\mathbf{z}^{k+1} - \mathbf{x}^\dagger\|_2 \leq \alpha \|\mathbf{z}^k - \mathbf{x}^\dagger\|_2 \leq \alpha \delta \|\mathbf{x}^\dagger\|_2 \leq \delta \|\mathbf{x}^\dagger\|_2$ for some $\alpha \in (0, 1)$. ■

Next we give the proof of second phase.

Proof: Given a vector \mathbf{z}^k satisfying $\mathbf{z}^k \in \mathcal{E}(\delta) \cap \mathcal{E}(\frac{x_{\min}^\dagger}{\|\mathbf{x}^\dagger\|_2})$ and a vector \mathbf{u}^k satisfying $\|\mathbf{u}^k - \mathbf{x}^\dagger\| \leq \rho \|\mathbf{z}^k - \mathbf{x}^\dagger\|$ where $\rho \in (0, 1)$, $\|\mathbf{u}^k\|_0 \leq s$ and $\mathcal{S}_{k+1} = \text{supp}(\mathbf{u}^k)$. Suppose that $\|\mathbf{z}^{k,0} - \mathbf{x}^\dagger\| \leq \|\mathbf{u}^k - \mathbf{x}^\dagger\|$ and $\text{supp}(\mathbf{z}^{k,0}) = \mathcal{S}_{k+1}$. Let $\mathcal{S}^\dagger := \text{supp}(\mathbf{x}^\dagger)$, $\mathcal{S}_k := \text{supp}(\mathbf{z}^k)$ and $\mathbf{h}^{k,0} := \mathbf{z}^{k,0} - \mathbf{x}^\dagger$. Assuming the event (IV.12) and (IV.13) holds.

We confirm that it holds $\mathcal{S}^\dagger \subseteq \mathcal{S}_{k+1}$ when $\|\mathbf{z}^{k,0} - \mathbf{x}^\dagger\|_2 < x_{\min}^\dagger$, otherwise there would exist an index $j \in \mathcal{S}^\dagger \setminus \mathcal{S}_{k+1} \neq \emptyset$, such that $\|\mathbf{z}^{k,0} - \mathbf{x}^\dagger\|_2 \geq |x_j| \geq x_{\min}^\dagger$, which contradicts with our assumption. Then we have

$$\|\mathbf{z}^{k,0} - \mathbf{x}^\dagger\|_2 \leq \|\mathbf{u}^k - \mathbf{x}^\dagger\|_2 \leq \rho \|\mathbf{z}^k - \mathbf{x}^\dagger\|_2 < x_{\min}^\dagger,$$

which implies that $\mathcal{S}^\dagger \subseteq \mathcal{S}_{k+1}$. Since $\mathbf{z}^k \in \mathcal{E}(\delta) \cap \mathcal{E}(\frac{x_{\min}^\dagger}{\|\mathbf{x}^\dagger\|_2})$, we obtain

$$(1 - \delta) \|\mathbf{x}^\dagger\|_2 \leq \|\mathbf{z}^{k,0}\|_2 \leq (1 + \delta) \|\mathbf{x}^\dagger\|_2.$$

In term of Lemma IV.2 with $\mathbf{z} = \mathbf{z}^{k,0}$ and $\mathcal{T} = \mathcal{S}_{k+1}$, we have

$$\begin{aligned} & \|(\mathbf{H}_{\mathcal{S}_{k+1}, \mathcal{S}_{k+1}}(\mathbf{z}^{k,0}))^{-1} \mathbf{J}_{\mathcal{S}_{k+1}}(\mathbf{z}^{k,0})^\top\|_2 \\ & \leq \frac{2}{\sqrt{2 - \delta(1 - \delta)} \|\mathbf{x}^\dagger\|_2}. \end{aligned} \quad (\text{IV.29})$$

Lemma IV.4 with $\mathbf{h} = \mathbf{h}^{k,0}$ and $\mathcal{T} = \mathcal{S}_{k+1}$ implies

$$\|\mathbf{J}_{\mathcal{S}_{k+1}}(\mathbf{h}^{k,0})\|_2 \leq \sqrt{2 + \frac{\delta}{4}} \|\mathbf{z}^{k,0} - \mathbf{x}^\dagger\|_2. \quad (\text{IV.30})$$

Similar to that in (IV.28), we can infer following equation

$$\begin{aligned} & \mathbf{H}_{\mathcal{S}_{k+1}, \mathcal{S}_{k+1}}(\mathbf{z}^{k,0})(\mathbf{z}_{\mathcal{S}_{k+1}}^{k+1} - \mathbf{x}_{\mathcal{S}_{k+1}}^\dagger) \\ & = \frac{1}{2} \mathbf{J}_{\mathcal{S}_{k+1}}(\mathbf{z}^{k,0})^\top \mathbf{J}_{\mathcal{S}_{k+1}}(\mathbf{h}^{k,0}) \mathbf{h}_{\mathcal{S}_{k+1}}^{k,0}, \end{aligned}$$

together with (IV.29) and (IV.30) yields that

$$\begin{aligned} & \|\mathbf{z}^{k+1} - \mathbf{x}^\dagger\|_2 \\ & = \|(\mathbf{H}_{\mathcal{S}_{k+1}, \mathcal{S}_{k+1}}(\mathbf{z}^{k,0}))^{-1} \mathbf{H}_{\mathcal{S}_{k+1}, \mathcal{S}_{k+1}}(\mathbf{z}^{k,0})(\mathbf{z}_{\mathcal{S}_{k+1}}^{k+1} - \mathbf{x}_{\mathcal{S}_{k+1}}^\dagger)\|_2 \|\boldsymbol{\varepsilon}\|_2 \leq C \|\mathbf{x}^\dagger\|_2 x_{\min}^\dagger. \\ & \leq \frac{1}{2} \|(\mathbf{H}_{\mathcal{S}_{k+1}, \mathcal{S}_{k+1}}(\mathbf{z}^{k,0}))^{-1} \mathbf{J}_{\mathcal{S}_{k+1}}(\mathbf{z}^{k,0})^\top \mathbf{J}_{\mathcal{S}_{k+1}}(\mathbf{h}^{k,0}) \mathbf{h}_{\mathcal{S}_{k+1}}^{k,0}\|_2 \\ & \leq \beta \|\mathbf{z}^k - \mathbf{x}^\dagger\|_2^2, \end{aligned}$$

where $\beta = \frac{\sqrt{8+\delta}}{2\sqrt{2-\delta(1-\delta)}\|\mathbf{x}^\dagger\|_2}$. ■

D. Proof of Corollary II.1

Proof: Given the initial estimate \mathbf{z}^0 satisfies $\mathbf{z}^0 \in \mathcal{E}(\delta)$ and \mathbf{z}^k is the k -th iteration point generated by Algorithm 1. Define $\mathcal{S}^\dagger := \text{supp}(\mathbf{x}^\dagger)$, $\mathcal{S}_k := \text{supp}(\mathbf{z}^k)$ and $\mathcal{T}_{k+1} := \mathcal{S}_k \cup \mathcal{S}_{k+1} \cup \mathcal{S}^\dagger$, which implies $|\mathcal{T}_{k+1}| \leq 3s$.

Assuming event (IV.12) and (IV.13) holds for K iterations, then according to Theorem II.1, there exist $\rho \in (0, 1)$ and $\alpha \in (0, 1)$ for any integer $0 \leq k \leq K$ such that:

$$\|\mathbf{u}^k - \mathbf{x}^\dagger\|_2 \leq \rho \|\mathbf{z}^k - \mathbf{x}^\dagger\|_2,$$

and

$$\|\mathbf{z}^{k+1} - \mathbf{x}^\dagger\|_2 \leq \alpha \|\mathbf{z}^k - \mathbf{x}^\dagger\|_2.$$

Let K_0 be the minimum integer such that

$$\delta \alpha^{K_0} \|\mathbf{x}^\dagger\|_2 < x_{\min}^\dagger.$$

We can show that $\mathcal{S}^\dagger \subseteq \mathcal{S}_k$ holds for all $k \geq K_0$ when $\|\mathbf{z}^k - \mathbf{x}^\dagger\|_2 \leq \delta \alpha^k \|\mathbf{x}^\dagger\|_2 \leq \delta \alpha^{K_0} \|\mathbf{x}^\dagger\|_2 < x_{\min}^\dagger$, otherwise there would exist an index $j \in \mathcal{S}^\dagger \setminus \mathcal{S}_k \neq \emptyset$, such that $\|\mathbf{z}^k - \mathbf{x}^\dagger\|_2 \geq |x_j| \geq x_{\min}^\dagger$, which contradicts with our assumption. Thus, we have

$$K_0 = \left\lfloor \frac{\log(\delta \|\mathbf{x}^\dagger\|_2 / x_{\min}^\dagger)}{\log(\alpha^{-1})} \right\rfloor + 1 \leq C_a \log(\|\mathbf{x}^\dagger\|_2 / x_{\min}^\dagger) + C_b.$$

where $\lfloor \cdot \rfloor$ denotes the floor operation and C_a, C_b are universal constants for fixed δ . Then for $k \geq K_0$, according to the result $\mathcal{S}^\dagger \subseteq \mathcal{S}_{k+1}$ and part b.) of Theorem II.1, we obtain

$$\|\mathbf{z}^{k+1} - \mathbf{x}^\dagger\|_2 \leq \beta \|\mathbf{z}^k - \mathbf{x}^\dagger\|_2^2, \quad (\text{IV.31})$$

where $\beta = \frac{\sqrt{8+\delta}}{2\sqrt{2-\delta(1-\delta)}\|\mathbf{x}^\dagger\|_2}$. Choosing $K = C_c \log \log(\|\mathbf{x}^\dagger\|_2 / \epsilon) + K_0$, and Theorem II.1 implies that $\beta \cdot \delta \|\mathbf{x}^\dagger\|_2 \leq 1$ as long as $\delta \in (0, 0.46)$, thus $\|\mathbf{z}^{k+1} - \mathbf{x}^\dagger\|_2 \leq \delta \|\mathbf{x}^\dagger\|_2$. Then with probability at least $1 - K(C_d m^{-1} - C_e \exp(-C_f m / \log m))$, we have

$$\begin{aligned} \|\mathbf{z}^K - \mathbf{x}^\dagger\|_2 & \leq \beta \cdot \|\mathbf{z}^{K-1} - \mathbf{x}^\dagger\|_2^2 \\ & \leq \beta^{2^{K-K_0-1}} \cdot \|\mathbf{z}^{K_0} - \mathbf{x}^\dagger\|_2^{2^{K-K_0}} \\ & \leq \beta^{2^{K-K_0-1}} \cdot (\delta \|\mathbf{x}^\dagger\|_2)^{2^{K-K_0}} \\ & \leq (\beta \cdot \delta \|\mathbf{x}^\dagger\|_2)^{2^{K-K_0}} \cdot \|\mathbf{x}^\dagger\|_2 \\ & \leq \epsilon \|\mathbf{x}^\dagger\|_2, \end{aligned}$$

provided $m \geq C_g K s \log(n/s)$. ■

E. Proof of Theorem II.2

First we give the proof of part a.) of the Theorem II.2.

Proof: In noisy case, $y_j := y_j^{(\varepsilon)} = |\langle \mathbf{a}_j, \mathbf{x}^\dagger \rangle|^2 + \varepsilon_j$, $j = 1, \dots, m$. Given \mathbf{z}^k satisfying $\|\mathbf{z}^k\|_0 \leq s$, $\mathbf{z}^k \in \mathcal{E}(\delta)$ and $\|\boldsymbol{\varepsilon}\|_2 \leq C \|\mathbf{x}^\dagger\|_2 x_{\min}^\dagger$. Let $\mathcal{S}^\dagger := \text{supp}(\mathbf{x}^\dagger)$, $\mathcal{S}_k := \text{supp}(\mathbf{z}^k)$ and $\mathcal{T}_{k+1} := \mathcal{S}_k \cup \mathcal{S}_{k+1} \cup \mathcal{S}^\dagger$, which indicates that $|\mathcal{T}_{k+1}| \leq 3s$. Assume that event (IV.12) and (IV.13) holds. Since

$$\begin{aligned} \mathbf{u}^k & = \mathcal{H}_s(\mathbf{z}^k - \mu^k \nabla f(\mathbf{z}^k)) \\ & = \mathcal{H}_s(\mathbf{z}^k - \mu^k \mathbf{J}(\mathbf{z}^k)^\top (\mathbf{J}(\mathbf{z}^k) + \mathbf{J}(\mathbf{x}^\dagger)) (\mathbf{z}^k - \mathbf{x}^\dagger) \\ & \quad - \mu^k \mathbf{J}(\mathbf{z}^k)^\top \boldsymbol{\varepsilon}), \end{aligned}$$

using the same argument to the proof of the inequality in part a.) of Theorem II.1, we obtain that

$$\begin{aligned} \|\mathbf{u}^k - \mathbf{x}^\dagger\|_2 & \leq \sqrt{\frac{3 + \sqrt{5}}{2}} (\mathbf{z}_{\mathcal{T}_{k+1}}^k - \mathbf{x}_{\mathcal{T}_{k+1}}^\dagger - \mu^k \nabla f_{\mathcal{T}_{k+1}}(\mathbf{z}^k)) \\ & \leq \rho \|\mathbf{z}^k - \mathbf{x}^\dagger\|_2 + p \|\boldsymbol{\varepsilon}\|_2, \end{aligned} \quad (\text{IV.32})$$

where $\rho = \sqrt{\frac{3 + \sqrt{5}}{2}} (1 - \mu^k \|\mathbf{x}^\dagger\|_2^2 (1 - \frac{9\delta}{2} - \frac{\delta^2}{4} - \frac{3\delta^3}{4}))$, $p = \sqrt{\frac{3 + \sqrt{5}}{2}} \mu^k \|\mathbf{x}^\dagger\|_2 \sqrt{2 + \frac{\delta}{4}} (1 + \delta)$ with

$\mu^k \in \left(\frac{2}{(8+\delta)(1+\delta)^2 \|\mathbf{x}^\dagger\|_2^2}, \frac{2}{(5+6\delta+7\delta^2) \|\mathbf{x}^\dagger\|_2^2} \right)$. Since $\|\varepsilon\| \leq C \|\mathbf{x}^\dagger\|_2 x_{\min}^\dagger$, then we have

$$\|\mathbf{u}^k - \mathbf{x}^\dagger\|_2 \leq \rho\delta \|\mathbf{x}^\dagger\|_2 + Cp \|\mathbf{x}^\dagger\|_2 \leq l \|\mathbf{x}^\dagger\|_2,$$

where $l = \rho\delta + Cp$. Then we have

$$(1-l) \|\mathbf{x}^\dagger\|_2 \leq \|\mathbf{u}^k\|_2 \leq (1+l) \|\mathbf{x}^\dagger\|_2.$$

We can choose proper parameters to ensure that $l \in (0, 1)$. For example, we can set $\mu^k \in (0.3966/\|\mathbf{x}^\dagger\|_2^2, 0.3975/\|\mathbf{x}^\dagger\|_2^2)$, such that $l \in (0, 1)$ if provided $C \leq 0.001$ and $\delta \leq 0.005$.

Then according to update rule in (II.10) for $L = 1$ and with the same argument to the proof of the first inequality in part b.) of Theorem II.1, we have

$$\begin{aligned} & \|\mathbf{z}_{S_{k+1}}^{k+1} - \mathbf{x}_{S_{k+1}}^\dagger\|_2 \\ & \leq \|\mathbf{u}_{S_{k+1}}^k - \mathbf{x}_{S_{k+1}}^\dagger - \frac{1}{2}(\mathbf{H}_{S_{k+1}}(\mathbf{u}^k))^{-1} \\ & \quad \cdot \mathbf{J}_{S_{k+1}}(\mathbf{u}^k)^\top (\mathbf{J}_{\mathcal{T}_{k+1}}(\mathbf{u}^k) \mathbf{u}_{\mathcal{T}_{k+1}}^k - \mathbf{J}_{\mathcal{T}_{k+1}}(\mathbf{x}^\dagger) \mathbf{x}_{\mathcal{T}_{k+1}}^\dagger)\|_2 \\ & \quad + \frac{1}{2} \|\varepsilon\|_2 \|(\mathbf{H}_{S_{k+1}}(\mathbf{u}^k))^{-1} \mathbf{J}_{S_{k+1}}(\mathbf{u}^k)^\top\|_2 \\ & \leq \xi_0 \|\mathbf{u}^k - \mathbf{x}^\dagger\|_2 + d \|\varepsilon\|_2, \end{aligned} \quad (\text{IV.33})$$

where $\xi_0 = \frac{\sqrt{(2-\delta)(8+\delta)l(1-l)+2\delta(1+l)^2}}{2(2-\delta)(1-l)^2}$ and $d = \frac{1}{\sqrt{2-\delta}(1-l)\|\mathbf{x}^\dagger\|_2}$. By (IV.32) and (IV.33) have

$$\|\mathbf{z}_{S_{k+1}}^{k+1} - \mathbf{x}_{S_{k+1}}^\dagger\|_2 \leq \xi_0 \rho \|\mathbf{z}^k - \mathbf{x}^\dagger\|_2 + (d + \xi_0 p) \|\varepsilon\|_2.$$

Since $\mathbf{x}_{S^\dagger \setminus S_{k+1}}^\dagger$ is a sub-vector of $\mathbf{u}_{\mathcal{T}_{k+1}}^k - \mathbf{x}_{\mathcal{T}_{k+1}}^\dagger$ and by $\sqrt{a^2 + b^2} \leq |a| + |b|$, we obtain

$$\begin{aligned} \|\mathbf{z}^{k+1} - \mathbf{x}^\dagger\|_2 &= \sqrt{\|\mathbf{x}_{S^\dagger \setminus S_{k+1}}^\dagger\|_2^2 + \|\mathbf{z}_{S_{k+1}}^{k+1} - \mathbf{x}_{S_{k+1}}^\dagger\|_2^2} \\ &\leq \sqrt{\|\mathbf{u}_{\mathcal{T}_{k+1}}^k - \mathbf{x}_{\mathcal{T}_{k+1}}^\dagger\|_2^2 + \|\mathbf{z}_{S_{k+1}}^{k+1} - \mathbf{x}_{S_{k+1}}^\dagger\|_2^2} \\ &\leq \xi \|\mathbf{z}^k - \mathbf{x}^\dagger\|_2 + \eta \|\varepsilon\|_2, \end{aligned}$$

where $\xi = \rho(1 + \xi_0)$ and $\eta = d + p(1 + \xi_0)$. Then according to the parameters chosen above, we have $\xi \in (0, 1)$. ■

Next we give the proof of part b.) of the Theorem II.2.

Proof: In noisy case, $y_j := y_j^{(\varepsilon)} = |\langle \mathbf{a}_j, \mathbf{x}^\dagger \rangle|^2 + \varepsilon_j$, $j = 1, \dots, m$. Given \mathbf{z}^k satisfying $\mathbf{z}^k \in \mathcal{E}(\delta) \cap \mathcal{E}(\frac{x_{\min}^\dagger}{\|\mathbf{x}^\dagger\|_2})$ and $\|\varepsilon\|_2 \leq C \|\mathbf{x}^\dagger\|_2 x_{\min}^\dagger$. Let $S^\dagger := \text{supp}(\mathbf{x}^\dagger)$, $S_k := \text{supp}(\mathbf{z}^k)$ and $\mathcal{T}_{k+1} := S_k \cup S_{k+1} \cup S^\dagger$, which indicates that $|\mathcal{T}_{k+1}| \leq 3s$. Assume that event (IV.12) and (IV.13) holds. Using the same argument to the proof of the inequality (IV.32), we have

$$\|\mathbf{u}^k - \mathbf{x}^\dagger\|_2 \leq \rho \|\mathbf{z}^k - \mathbf{x}^\dagger\|_2 + p \|\varepsilon\|_2. \quad (\text{IV.34})$$

where $\rho = \sqrt{\frac{3+\sqrt{5}}{2}}(1 - \mu^k \|\mathbf{x}^\dagger\|_2^2(1 - \frac{9\delta}{2} - \frac{\delta^2}{4} - \frac{3\delta^3}{4}))$, $p = \sqrt{\frac{3+\sqrt{5}}{2}} \mu^k \|\mathbf{x}^\dagger\|_2 \sqrt{2 + \frac{\delta}{4}(1 + \delta)}$ with $\mu^k \in \left(\frac{2}{(8+\delta)(1+\delta)^2 \|\mathbf{x}^\dagger\|_2^2}, \frac{2}{(5+6\delta+7\delta^2) \|\mathbf{x}^\dagger\|_2^2} \right)$. Since $\mathbf{z}^k \in \mathcal{E}(\delta) \cap \mathcal{E}(\frac{x_{\min}^\dagger}{\|\mathbf{x}^\dagger\|_2})$ and $\|\varepsilon\| \leq C \|\mathbf{x}^\dagger\|_2 x_{\min}^\dagger$, we have

$$\|\mathbf{u}^k - \mathbf{x}^\dagger\|_2 \leq \rho \|\mathbf{z}^k - \mathbf{x}^\dagger\|_2 + p \|\varepsilon\|_2 \leq l \cdot x_{\min}^\dagger,$$

which implies

$$(1-l) \|\mathbf{x}^\dagger\|_2 \leq \|\mathbf{u}^k\|_2 \leq (1+l) \|\mathbf{x}^\dagger\|_2,$$

where $l = \rho + Cp$. We can choose proper parameters to ensure that $l \in (0, 1)$. For example, we can set $\mu^k \in (0.3960/\|\mathbf{x}^\dagger\|_2^2, 0.3975/\|\mathbf{x}^\dagger\|_2^2)$, such that $l \in (0, 1)$ if provided $C = 0.001$ and $\delta \leq 0.005$.

With the same argument to the proof of part b.) of Theorem II.1, we confirm that it holds $S^\dagger \subseteq S_{k+1}$ since we have

$$\|\mathbf{u}^k - \mathbf{x}^\dagger\|_2 \leq l \cdot x_{\min}^\dagger < x_{\min}^\dagger.$$

Then we obtain that

$$\begin{aligned} & \|\mathbf{z}^{k+1} - \mathbf{x}^\dagger\|_2 \\ & \leq \frac{1}{2} \|(\mathbf{H}_{S_{k+1}}(\mathbf{u}^k))^{-1} \mathbf{J}_{S_{k+1}}(\mathbf{u}^k)^\top \\ & \quad \cdot (\mathbf{J}_{S_{k+1}}(\mathbf{u}^k) - \mathbf{J}_{S_{k+1}}(\mathbf{x}^\dagger))(\mathbf{u}_{S_{k+1}}^k - \mathbf{x}_{S_{k+1}}^\dagger)\|_2 \\ & \quad + \frac{1}{2} \|\varepsilon\|_2 \|(\mathbf{H}_{S_{k+1}}(\mathbf{u}^k))^{-1} \mathbf{J}_{S_{k+1}}(\mathbf{u}^k)^\top\|_2 \\ & \leq \zeta_0 \|\mathbf{u}^k - \mathbf{x}^\dagger\|_2^2 + d \|\varepsilon\|_2, \end{aligned} \quad (\text{IV.35})$$

where $\zeta_0 = \frac{\sqrt{8+\delta}}{2\sqrt{2-\delta}(1-l)\|\mathbf{x}^\dagger\|_2}$ and $d = \frac{1}{\sqrt{2-\delta}(1-l)\|\mathbf{x}^\dagger\|_2}$. By substituting (IV.34) into (IV.35) we have

$$\|\mathbf{z}^{k+1} - \mathbf{x}^\dagger\|_2 \leq \zeta \|\mathbf{z}^k - \mathbf{x}^\dagger\|_2^2 + \gamma \|\varepsilon\|_2,$$

where $\zeta = \zeta_0 \rho^2$ and $\gamma = \frac{(2\rho\delta + Cp)p\sqrt{8+\delta}}{2\sqrt{2-\delta}(1-l)} + d$. ■

REFERENCES

- [1] A. Walther, "The question of phase retrieval in optics," *Optica Acta: International Journal of Optics*, vol. 10, no. 1, pp. 41–49, 1963.
- [2] Y. Shechtman, Y. C. Eldar, O. Cohen, H. N. Chapman, J. Miao, and M. Segev, "Phase retrieval with application to optical imaging: a contemporary overview," *IEEE Signal Processing Magazine*, vol. 32, no. 3, pp. 87–109, 2015.
- [3] R. W. Harrison, "Phase problem in crystallography," *JOSA a*, vol. 10, no. 5, pp. 1046–1055, 1993.
- [4] H. Reichenbach, *Philosophic foundations of quantum mechanics*. Courier Corporation, 1998.
- [5] T. Heinosaari, L. Mazzarella, and M. M. Wolf, "Quantum tomography under prior information," *Communications in Mathematical Physics*, vol. 318, no. 2, pp. 355–374, 2013.
- [6] C. Fienup and J. Dainty, "Phase retrieval and image reconstruction for astronomy," *Image Recovery: Theory and Application*, vol. 231, p. 275, 1987.
- [7] J. Miao, T. Ishikawa, Q. Shen, and T. Earnest, "Extending x-ray crystallography to allow the imaging of noncrystalline materials, cells, and single protein complexes," *Annu. Rev. Phys. Chem.*, vol. 59, pp. 387–410, 2008.
- [8] E. J. Candes, Y. C. Eldar, T. Strohmer, and V. Voroninski, "Phase retrieval via matrix completion," *SIAM Review*, vol. 57, no. 2, pp. 225–251, 2015.
- [9] G. Wang, L. Zhang, G. B. Giannakis, M. Akçakaya, and J. Chen, "Sparse phase retrieval via truncated amplitude flow," *IEEE Transactions on Signal Processing*, vol. 66, no. 2, pp. 479–491, 2017.
- [10] R. Balan, P. Casazza, and D. Edidin, "On signal reconstruction without phase," *Applied and Computational Harmonic Analysis*, vol. 20, no. 3, pp. 345–356, 2006.
- [11] A. Conca, D. Edidin, M. Hering, and C. Vinzant, "An algebraic characterization of injectivity in phase retrieval," *Applied and Computational Harmonic Analysis*, vol. 38, no. 2, pp. 346–356, 2015.
- [12] R. Gerhberg and W. Saxton, "A practical algorithm for the determination of phase from image and diffraction plane picture," *Optik*, vol. 35, pp. 237–246, 1972.
- [13] J. R. Fienup, "Phase retrieval algorithms: a comparison," *Applied optics*, vol. 21, no. 15, pp. 2758–2769, 1982.

- [14] E. J. Candes, T. Strohmer, and V. Voroninski, "Phaselift: Exact and stable signal recovery from magnitude measurements via convex programming," *Communications on Pure and Applied Mathematics*, vol. 66, no. 8, pp. 1241–1274, 2013.
- [15] I. Waldspurger, A. d'Aspremont, and S. Mallat, "Phase recovery, maxcut and complex semidefinite programming," *Mathematical Programming*, vol. 149, pp. 47–81, 2015.
- [16] T. Goldstein and C. Studer, "Phasemax: Convex phase retrieval via basis pursuit," *IEEE Transactions on Information Theory*, vol. 64, no. 4, pp. 2675–2689, 2018.
- [17] S. Bahmani and J. Romberg, "A flexible convex relaxation for phase retrieval," *Electronic Journal of Statistics*, vol. 11, no. 2, pp. 5254–5281, 2017.
- [18] P. Netrapalli, P. Jain, and S. Sanghavi, "Phase retrieval using alternating minimization," *Advances in Neural Information Processing Systems*, vol. 26, 2013.
- [19] E. J. Candes, X. Li, and M. Soltanolkotabi, "Phase retrieval via wirtinger flow: Theory and algorithms," *IEEE Transactions on Information Theory*, vol. 61, no. 4, pp. 1985–2007, 2015.
- [20] G. Wang, G. B. Giannakis, and Y. C. Eldar, "Solving systems of random quadratic equations via truncated amplitude flow," *IEEE Transactions on Information Theory*, vol. 64, no. 2, pp. 773–794, 2017.
- [21] K. Wei, "Solving systems of phaseless equations via kacmarz methods: A proof of concept study," *Inverse Problems*, vol. 31, no. 12, p. 125008, 2015.
- [22] Y. S. Tan and R. Vershynin, "Phase retrieval via randomized kacmarz: theoretical guarantees," *Information and Inference: A Journal of the IMA*, vol. 8, no. 1, pp. 97–123, 2019.
- [23] J. Cai and K. Wei, "Solving systems of phaseless equations via riemannian optimization with optimal sampling complexity," *Journal of Computational Mathematics*, vol. 42, no. 3, pp. 755–783, 2024. [Online]. Available: <https://doi.org/10.4208/jcm.2207-m2021-0247>
- [24] B. Gao and Z. Xu, "Phaseless recovery using the gauss–newton method," *IEEE Transactions on Signal Processing*, vol. 65, no. 22, pp. 5885–5896, 2017.
- [25] C. Ma, X. Liu, and Z. Wen, "Globally convergent levenberg-marquardt method for phase retrieval," *IEEE Transactions on Information Theory*, vol. 65, no. 4, pp. 2343–2359, 2018.
- [26] LI, L. Hui-Ping, and Song, "Phase retrieval with phaselift algorithm," *Applied Mathematics: A Journal of Chinese Universities*, vol. v.35, no. 04, pp. 104–127, 2020.
- [27] H. Li, S. Li, and Y. Xia, "Sampling complexity on phase retrieval from masked fourier measurements via wirtinger flow," *Inverse Problems*, vol. 38, no. 10, p. 105004, 2022.
- [28] S. Mallat, *A wavelet tour of signal processing*. Elsevier, 1999.
- [29] Y. Wang and Z. Xu, "Phase retrieval for sparse signals," *Applied and Computational Harmonic Analysis*, vol. 37, no. 3, pp. 531–544, 2014.
- [30] M. Akçakaya and V. Tarokh, "Sparse signal recovery from a mixture of linear and magnitude-only measurements," *IEEE Signal Processing Letters*, vol. 22, no. 9, pp. 1220–1223, 2015.
- [31] X. Li and V. Voroninski, "Sparse signal recovery from quadratic measurements via convex programming," *SIAM Journal on Mathematical Analysis*, vol. 45, no. 5, pp. 3019–3033, 2013.
- [32] G. Jagatap and C. Hegde, "Sample-efficient algorithms for recovering structured signals from magnitude-only measurements," *IEEE Transactions on Information Theory*, vol. 65, no. 7, pp. 4434–4456, 2019.
- [33] T. T. Cai, X. Li, and Z. Ma, "Optimal rates of convergence for noisy sparse phase retrieval via thresholded wirtinger flow," *The Annals of Statistics*, vol. 44, no. 5, pp. 2221–2251, 2016.
- [34] M. Soltanolkotabi, "Structured signal recovery from quadratic measurements: Breaking sample complexity barriers via nonconvex optimization," *IEEE Transactions on Information Theory*, vol. 65, no. 4, pp. 2374–2400, 2019.
- [35] J.-F. Cai, Y. Jiao, X. Lu, and J. You, "Sample-efficient sparse phase retrieval via stochastic alternating minimization," *IEEE Transactions on Signal Processing*, vol. 70, pp. 4951–4966, 2022.
- [36] J.-F. Cai, J. Li, X. Lu, and J. You, "Sparse signal recovery from phaseless measurements via hard thresholding pursuit," *Applied and Computational Harmonic Analysis*, vol. 56, pp. 367–390, 2022.
- [37] J.-F. CAI, Y. Long, R. WEN, and J. Ying, "A fast and provable algorithm for sparse phase retrieval," in *The Twelfth International Conference on Learning Representations*, 2024. [Online]. Available: <https://openreview.net/forum?id=Blkxb16vzl>
- [38] J.-F. Cai, J. Li, and J. You, "Provable sample-efficient sparse phase retrieval initialized by truncated power method," *Inverse Problems*, vol. 39, no. 7, p. 075008, 2023.
- [39] M. Xu, D. Dong, and J. Wang, "Subspace phase retrieval," *IEEE Transactions on Information Theory*, 2024.
- [40] X. Yuan, P. Li, and T. Zhang, "Exact recovery of hard thresholding pursuit," *Advances in Neural Information Processing Systems*, vol. 29, 2016.
- [41] X.-T. Yuan, P. Li, and T. Zhang, "Gradient hard thresholding pursuit," *Journal of Machine Learning Research*, vol. 18, no. 166, pp. 1–43, 2018.
- [42] S. Foucart, "Hard thresholding pursuit: an algorithm for compressive sensing," *SIAM Journal on Numerical Analysis*, vol. 49, no. 6, pp. 2543–2563, 2011.
- [43] Å. Björck, *Numerical methods for least squares problems*. SIAM, 1996.
- [44] R. Fletcher, *Practical methods of optimization*. John Wiley & Sons, 2000.
- [45] Y. Chen and E. Candes, "Solving random quadratic systems of equations is nearly as easy as solving linear systems," *Advances in Neural Information Processing Systems*, vol. 28, 2015.
- [46] J. Sun, Q. Qu, and J. Wright, "A geometric analysis of phase retrieval," *Foundations of Computational Mathematics*, vol. 18, pp. 1131–1198, 2018.
- [47] J. Shen and P. Li, "A tight bound of hard thresholding," *Journal of Machine Learning Research*, vol. 18, no. 208, pp. 1–42, 2018.